FIELD EXPERIMENTS AND SIMULATIONS OF INFILTRATION-RATE RESPONSE TO CHANGES IN HYDROLOGIC CONDITIONS FOR AN ARTIFICIAL-RECHARGE TEST BASIN NEAR OAKES, SOUTHEASTERN NORTH DAKOTA

By D. M. Sumner, U.S. Geological Survey,
W. M. Schuh, North Dakota State Water Commission, and
R. L. Cline, North Dakota State Water Commission

U.S. GEOLOGICAL SURVEY
Water-Resources Investigations Report 91-4127

Prepared by the U.S. GEOLOGICAL SURVEY
in cooperation with the
NORTH DAKOTA STATE WATER COMMISSION and the
U.S. BUREAU OF RECLAMATION

Bismarck, North Dakota
1991

U.S. DEPARTMENT OF THE INTERIOR

MANUEL LUJAN, JR., Secretary

U.S. GEOLOGICAL SURVEY

Dallas L. Peck, Director

For additional information
write to:

District Chief
U.S. Geological Survey
Water Resources Division
821 East Interstate Avenue
Bismarck, ND 58501

Copies of this report can be
purchased from:

U.S. Geological Survey
Books and Open-File Reports
Federal Center
Box 25425
Denver, CO 80225

CONTENTS

ILLUSTRATIONS

ILLUSTRATIONS, Continued

TABLES

CONVERSION FACTORS AND ABBREVIATED WATER-QUALITY UNITS

Multiply	By	To obtain
centimeter (cm)	0.394	inch
centimeter per hour (cm/h)	0.783	foot per day
cubic meter per day (m^3/d)	35.32	cubic foot per day
gram per cubic centimeter (g/cm^3)	0.0361	pound per cubic inch
hectare (ha)	2.47	acre
meter (m)	3.281	foot
meter per day (m/d)	3.281	foot per day
cubic meter per day per square meter times meter of aquifer thickness $[(m^3/d)/m^2]m$	10.76	cubic foot per day per square foot times foot of aquifer thickness

Milligrams per liter (mg/L) is a unit expressing the concentration of a chemical constituent in solution as weight (milligrams) of solute per unit volume (liter) of water: 1 mg/L equals 1,000 micrograms per liter (µg/L).

FIELD EXPERIMENTS AND SIMULATIONS OF INFILTRATION-RATE RESPONSE TO CHANGES IN HYDROLOGIC CONDITIONS FOR AN ARTIFICIAL-RECHARGE TEST BASIN NEAR OAKES, SOUTHEASTERN NORTH DAKOTA

By
D. M. Sumner, U.S. Geological Survey,
W. M. Schuh, North Dakota State Water Commission,
and
R. L. Cline, North Dakota State Water Commission

ABSTRACT

Ponded depth in an artificial-recharge basin was used as a management option to conduct turbid water from the James River to the Oakes aquifer. Infiltration-rate response to changes in ponded depth was evaluated for a 15x15-meter artificial-recharge test basin constructed in a medium-sandy soil in the irrigation area near Oakes, southeastern North Dakota. Field experiments conducted at the test basin indicated that the clogged soil surface was easily scoured by currents caused by the addition of turbid water to increase ponded depth. Field measurements and computer-model simulations indicated that infiltration-rate response to an increase in ponded depth would be large for a clogged soil condition consisting of a surface filter-cake layer 0.1 centimeter in depth underlain by a sediment-clogged layer extending from 0.1 to 23 centimeters beneath the basin floor. Simulated infiltration-rate response to changes in ponded depth for surface filter-cake layer impedance values ranging from 0 to 1,000 hours indicated that infiltration-rate response would approach and remain near the maximum value for impedance values greater than 10 hours. The smallest infiltration-rate response would occur for impedance values less than 1 hour. For the case of a ground-water mound intersecting the basin floor, the percentage of infiltration-rate response to changes in ponded depth was not influenced by basin geometry, basin surface area, or underlying aquifer hydraulic conductivity. The simulated infiltration-rate response to changes in ponded depth increased when the water-table depth was shallow. Total recharge per unit area was greater for artificial-recharge basins having a less compact geometry than for artificial-recharge basins having a more compact geometry, for artificial-recharge basins having a small surface area than for artificial-recharge basins having a large surface area, and for artificial-recharge basins where underlying aquifer hydraulic conductivity was large rather than small. Artificial-recharge basin conditions most conducive to an effective infiltration-rate response to changes in ponded depth were least conducive to an enhanced total recharge.

INTRODUCTION

The irrigation area located near Oakes in southeastern North Dakota is part of the Garrison Diversion Unit project authorized by Congress in 1965. A component of the Garrison Diversion Unit project calls for the diversion of Missouri River water eastward to the James River via the McClusky Canal, the Lonetree Reservoir, the New Rockford Canal, and the James River feeder canal for irrigation. Because channel capacity of the James River is insufficient to meet peak irrigation demands for the irrigation area near Oakes, the U.S. Bureau of Reclamation proposed construction of Lake Taayer Reservoir.

In 1984, Congress passed Public Law 98-360, section 207, which required the appointment of a 12-member commission by the Secretary of the Interior to "examine, review, evaluate, and make recommendations with regard to the contemporary water-development needs of the State of North Dakota." Recommendations of the commission concerning irrigation in the Oakes area included the assessment of the feasibility of artificial recharge to the Oakes aquifer as an alternative to the Lake Taayer Reservoir.

In July 1985, the U.S. Geological Survey and the North Dakota State Water Commission entered into a cooperative agreement with the U.S. Bureau of Reclamation to investigate the feasibility of artificial recharge to the Oakes aquifer. Phase I of the feasibility study describes the geometric, hydraulic, and hydrochemical properties of the Oakes aquifer. Results of phase I were presented by Shaver and Schuh (1990), and data for phase I were presented by Shaver and Hove (1990).

Phase II of the feasibility study describes the selection, construction, maintenance, and performance evaluation of two artificial-recharge test basins in the irrigation area near Oakes. The test basins were operated from September 1986 to October 1987. Phase II investigations included a detailed evaluation of physical and hydraulic changes caused by the addition of turbid James River water to the medium-sandy test-basin soil during the following conditions: (1) Full renovation (complete removal of soil clogged during previous test-basin operations), (2) natural renovation through drying (allowing clogged soil to remain in place but allowing a period of drying to cause cracks in the clogged soil), and (3) the use of an organic mat surface filter. Results of the detailed evaluation were presented by Schuh and Shaver (1988).

Phase III of the feasibility study describes a preliminary cost analysis of full-project-scale and pilot-scale well fields and of artificial-recharge test basins for the Oakes aquifer. Results of phase III were presented by Shaver (1989).

Part of the phase II investigations included a detailed evaluation of infiltration-rate response to changes in ponded depth. Infiltration-rate response to changes in ponded depth is very complex and can be influenced by many factors including the homogeneity of the basin soil, the strength and

elasticity of the soil grain matrix, the depth of the underlying aquifer, the extent of ground-water mounding during basin operation, and the physical and hydraulic changes in the basin soil caused by the addition of turbid water.

The purpose of this study was to evaluate the relative efficiency of using deep and shallow ponded depths in an artificial-recharge basin as a management option to conduct turbid water from the James River to the Oakes aquifer. Infiltration-rate response to changes in ponded depth was evaluated for an artificial-recharge test basin in the irrigation area near Oakes (fig. 1). This report presents the results of the detailed evaluation. Evaluations in this report are based on: (1) Field experiments conducted at artificial-recharge test basins in the Oakes area, (2) computer simulations based on hydraulic data measured during test-basin operation, and (3) soil and water chemistry data measured during test-basin operation and published by Huff and Wald (1989).

INFILTRATION-RATE RESPONSE

Factors Affecting Infiltration-Rate Response

Infiltration-rate (i) response to changes in ponded depth (H) is largely variable and depends on the homogeneity of hydraulic properties of the unsaturated zone, basin design and geometry, and characteristics of the underlying aquifer. Response also varies with water-detention time in a basin because of hydraulic-conductivity changes caused by sediment and by biological and chemical constituents of the influent water.

For artificial recharge of an aquifer underlain by an impermeable substratum, Bouwer (1969) discussed i response to changes in H for two distinct cases. The first case (fig. 2, case A) is that of infiltration through a nonhomogeneous unsaturated zone in which an impeding surface soil layer causes desaturation of the soil between the impeding layer and the water table. The impeding material may consist of a natural preexisting soil. Frequently, however, the impeding surface layer is formed or is strongly enhanced by changes in the basin soil that are caused by basin operation.

The addition of turbid water to a basin commonly results in deposition of clay within the soil pores to depths varying from 1 to 38 cm and in formation of a surface filter-cake layer (Goss and others, 1973; Dilyunas, 1976; Schuh, 1988). The surface filter-cake layer is formed by silt particles straining out on the surface of the basin sand and is composed of silt particles as well as clay particles intercepted by the silt particles during late stages of basin operation (Schuh, 1988). Sediment clogging within the soil grain matrix commonly results in hydraulic-impedance values 10 to 100 times those of the initial soil (Dilyunas, 1976; Schuh, 1988). Surface filter-cake layers commonly reach impedance values two to five orders of magnitude greater than the impedance values of nonclogged basin subsoil (Dilyunas, 1976; Schuh, 1988; Schuh and Shaver, 1988). The impedance changes, in turn, affect i response to changes in H.

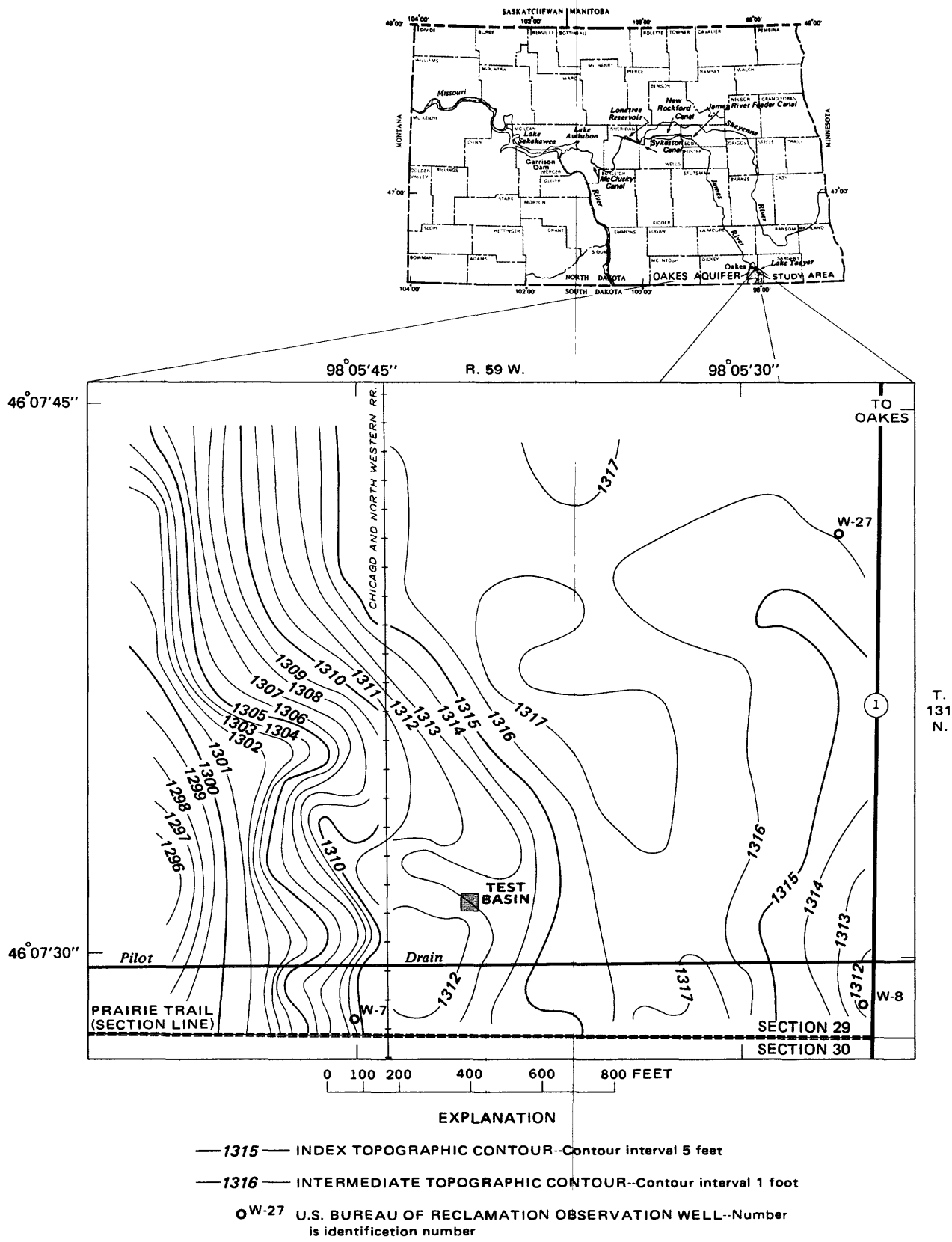

Figure 1.--Location of test basin. [Modified from Schuh and Shaver, 1988.]

CASE A

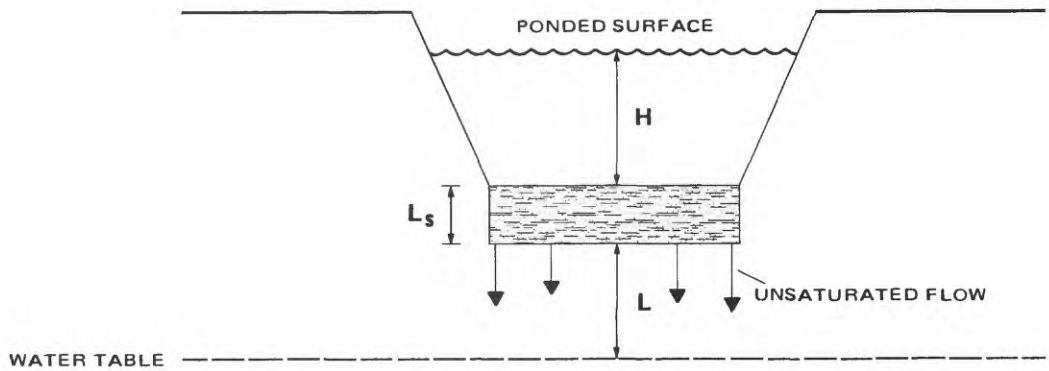

VERTICAL UNSATURATED FLOW THROUGH AN IMPEDING SURFACE SOIL LAYER

CASE B

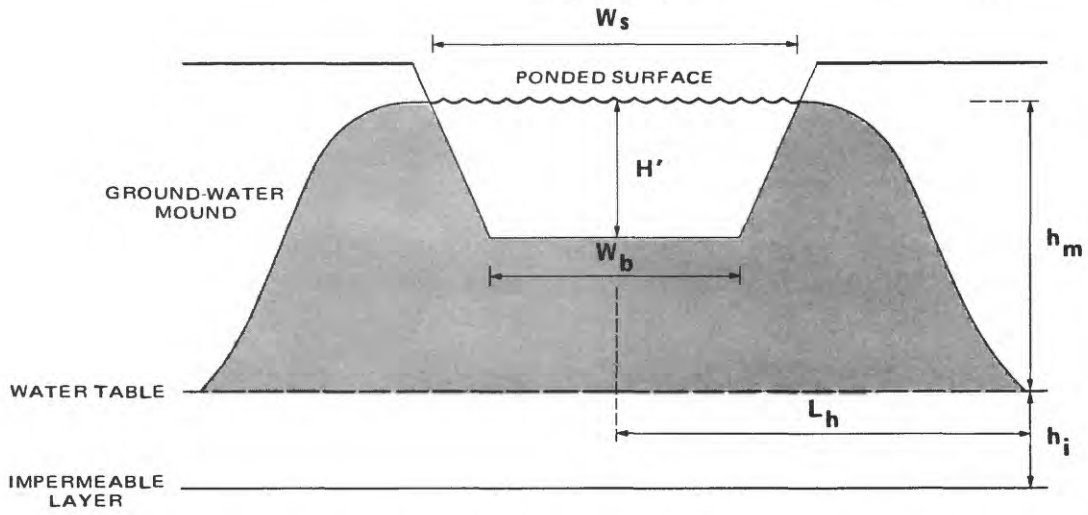

HORIZONTAL SATURATED FLOW DURING CONDITIONS OF GROUND-WATER MOUNDING

EXPLANATION

H	PONDED DEPTH, IN CENTIMETERS
L_s	THICKNESS OF SURFACE SOIL LAYER, IN CENTIMETERS
L	THICKNESS OF UNSATURATED ZONE, IN CENTIMETERS
W_s	WIDTH OF CHANNEL AT SURFACE OF PONDED WATER, IN METERS
H'	PONDED DEPTH, IN METERS
h_m	HEIGHT OF GROUND-WATER MOUND ABOVE INITIAL WATER TABLE, IN METERS
W_b	WIDTH OF CHANNEL AT BOTTOM OF PONDED WATER, IN METERS
h_i	SATURATED THICKNESS OF UNDERLYING AQUIFER BEFORE GROUND-WATER MOUND FORMATION, IN METERS
L_h	DISTANCE FROM CENTER OF CHANNEL TO POSITION WHERE GROUND-WATER MOUND HEIGHT EFFECTS ARE NEGLIGIBLE, IN METERS

Figure 2.--Spatial parameters for vertical unsaturated flow through an impeding surface soil layer and for horizontal saturated flow during conditions of ground-water mounding.

Basin soil impedance also can be increased by biological processes. Allison (1947) and Nevo and Mitchell (1967) described soil clogging caused by the formation of microbial gums. Bouwer and Rice (1989) described surface clogging caused by the deposition of algae and documented secondary effects caused by increased water-detention times in deep basins. Water cycling through the basin at a slower rate resulted in increased algae populations that, in turn, caused an increase in algal photosynthesis. The increase in algal photosynthesis caused an increase in water pH that, in turn, caused calcium-carbonate precipitation on the basin floor. The result was a net decrease in i following an increase in H.

For case A (fig. 2), Darcy's law for one-dimensional steady-state vertical flow through a homogeneous soil layer is used to calculate i response to changes in H:

$$i = \frac{K\,(H - S + L_S)}{L_S}, \qquad (1)$$

where

i = infiltration rate, in centimeters per hour;
K = hydraulic conductivity, in centimeters per hour (applied in this case for lower boundary of surface soil layer);
H = ponded depth, in centimeters;
S = pore-water pressure head, in centimeters of water (defined in this case for lower boundary of surface soil layer); and
L_S = thickness of surface soil layer, in centimeters.

The magnitude of i response to changes in H is dependent upon the negative pore-water pressure head (S) at the lower boundary of the surface soil layer and upon the thickness of the surface soil layer (L_S). If H is very large in relation to S and L_S, then i response to changes in H will approach a 1:1 proportionality. If H is small in relation to S and L_S, then i response to changes in H will be negligible.

The second case (fig. 2, case B) occurs when the geometry of an artificial-recharge basin is sufficiently compact, the surface area of an artificial-recharge basin is sufficiently large, and the transmissivity of an underlying aquifer is sufficiently small in relation to the basin infiltration rate that a ground-water mound intersects the basin floor during early stages of basin operation. For this case, equation 1 cannot be used to evaluate i response to changes in H. Equations describing the formation and dissipation of a ground-water mound have been developed by Hantush (1967) and others.

Bouwer (1969) used detailed resistance analog analyses and simplified Dupuit-Forchheimer assumptions to describe infiltration through a channel surface. If the width of the channel at the bottom of the ponded water (W_b) is large in relation to the saturated thickness of the underlying aquifer before ground-water mound formation [h_i; $h_i/W_b < 3$; Bouwer, 1969] and if the diameter of the ground-water mound is such that lateral flow is predominant,

infiltration-rate response to changes in ponded depth can be calculated with the following equation:

$$\frac{i'}{K'} = \frac{2\ h_m}{W_s}\ \frac{H' + h_i - 0.5\ h_m}{L_h - 0.25\ (W_b + W_s)}, \qquad (2)$$

where

i' = infiltration rate, in meters per day;
h_m = height of ground-water mound above initial water table, in meters;
H' = ponded depth, in meters;
h_i = saturated thickness of underlying aquifer before ground-water mound formation, in meters;
K' = hydraulic conductivity, in meters per day;
W_s = width of channel at surface of ponded water, in meters;
L_h = distance from center of channel to position where ground-water mound height effects are negligible, in meters; and
W_b = width of channel at bottom of ponded water, in meters.

However, this simplified relation applies only to a channel of infinite length in relation to width and cannot be applied with confidence to surface geometries of most basins.

The use of meter length units in equation 2, following the use of centimeter length units in equation 1, is made on the basis of appropriate spatial scale for each applied model. Applications of Darcy's law for unsaturated-flow models usually require small length scales. It is, therefore, appropriate to use centimeter length units for unsaturated-flow model applications and for presentation of the modeling results. Saturated-flow models usually require much larger length scales and much faster flow rates. It is, therefore, appropriate to use meter length units for saturated-flow model applications and for presentation of the modeling results. The use of centimeter length units for unsaturated-flow model applications and for presentation of the modeling results and meter length units for saturated-flow model applications and for presentation of the modeling results is maintained throughout this report.

Other factors affecting i response to changes in H include increased infiltration surface caused by the addition of nonlined basin-wall area to the total wetted surface (Jones and others, 1974) and compression of the basin soil, particularly the surface filter-cake layer, caused by increased effective stress from the weight of additional ponded water (Bouwer and Rice, 1989). Baumann (1965) suggested that increasing H to more than 120 cm would cause increased risk of consolidation. In addition, Suter and Harmeson (1960) stated that the surface filter-cake layer can be scoured easily by currents. In some cases, scouring by currents caused by the addition of turbid water to increase H can result in a larger than 1:1 i response to changes in H.

Comparative Index

In order to compare infiltration-rate (i) response to changes in ponded depth (H) for varying basin operations, a quantitative index is required. For this purpose, an infiltration-rate response ratio (τ) is calculated with the following equation:

$$\tau = \frac{(i_2/i_1)}{(H_2/H_1)}, \qquad (3)$$

where

τ = infiltration-rate response ratio, dimensionless;
i_2 = final infiltration rate, in centimeters per hour;
i_1 = initial infiltration rate, in centimeters per hour;
H_2 = final ponded depth, in centimeters; and
H_1 = initial ponded depth, in centimeters.

τ was used for all field-experiment comparisons of i response to changes in H and for all computer-simulation comparisons of i response to changes in H.

In practical terms, τ can be interpreted as follows. If τ equals 1, i response to changes in H is a 1:1 proportional relation. This means that i is optimally responsive to H within the H, pore-water pressure head (S), and thickness of surface soil layer (L_S) pressure head components described in equation 1 and that i response virtually is controlled hydraulically by changes in H. In the case where τ equals 1, increasing H would be most beneficial, providing that other indirect effects of H (such as consolidation or biochemically induced clogging) do not override the direct hydraulic benefits.

If τ is greater than 1, i response to changes in H is greater than 1:1. This means that i response is greater than could be attributed to optimal hydraulic response based on Darcian behavior (described in eq. 1). Such an increase in i can only be attributed to a change in hydraulic conductivity (K). The change in K, in turn, must be caused by some form of disturbance, such as perturbation of a sealing layer by currents caused by influent water. Even though increases in i under such conditions might be large, their dependence upon external perturbation indicates that they are not quantitatively predictable and are likely to be transitory.

If τ is less than 1, i response is determined largely by head components (eq. 1) other than H. Such diminished sensitivity means that increases in H are less likely to provide a substantial increase in recharge. This general response trend is indicated qualitatively for all cases where τ is less than 1. However, τ can be used as a quantitative scale of the sensitivity of i to H only if a fixed proportion of H values is used for analytical comparison. This is necessary because, although the maximum hydraulic-response value of τ is always 1 (provided there is not perturbation), the lowest value of τ (indicating no i response to changes in H) depends on the proportion of final

ponded depth (H_2) to initial ponded depth (H_1). For example, if H_2 divided by H_1 equals 2, the minimum τ value (indicating no response) is 0.5. However, if H_2 divided by H_1 equals 4, the minimum τ value is 0.25. The use of τ as a quantitative scale, then, requires a similar proportion of H_2 to H_1 between comparisons. For our application, all model comparisons use H_2 divided by H_1 equals 2, and all field measurements attempt to approach H_2 divided by H_1 equals 2 as closely as possible. Comparisons made in this study thus span from nonresponse of i to changes in H at τ equals 0.5 to a linear response at τ equals 1.

For a saturated surface soil layer having a constant known thickness, a constant K, and a known S at the lower boundary, τ can be calculated by combining equations 1 and 3:

$$\tau = \frac{H_1}{H_2} \frac{(H_2 - S_2 + L_s)}{(H_1 - S_1 + L_s)}, \qquad (4)$$

where

S_2 = final pore-water pressure head at lower boundary of surface soil layer, in centimeters of water; and
S_1 = initial pore-water pressure head at lower boundary of surface soil layer, in centimeters of water.

However, because S at the lower boundary of the surface soil layer was not known and could not be estimated easily for a multilayered soil, i response to changes in H during early stages of basin operation was simulated with a model based on the one-dimensional vertical transient-flow equation:

$$c(s) \frac{\partial S}{\partial t} = \frac{\partial}{\partial z} [K(S) (\frac{\partial S}{\partial z} + 1)], \qquad (5)$$

where

$c(s)$ = specific-moisture capacity, in inverse centimeters;
$K(S)$ = unsaturated hydraulic conductivity, in centimeters per hour;
t = time, in hours; and
z = depth coordinate, in centimeters.

Soil hydraulic parameters measured in the field during the test-basin clogging process were used in the computer simulations. A computer simulation of i response to changes in H for late stages of basin operation enabled a direct comparison of computer-simulation results with field-experiment results and provided a means of assessing the accuracy of the model. The model used is described in greater detail in the section titled "Model Development."

Neither the field-experiment results nor the one-dimensional vertical transient-flow model could be used to evaluate the case where a ground-water mound intersects the basin floor during early stages of basin operation (fig. 2, case B). Moreover, the simplified Dupuit-Forchheimer analysis

described in equation 2 is inappropriate for the finite lengths of most artificial-recharge basins. For case B (fig. 2), i response to changes in H can be simulated with a model based on the two-dimensional saturated unconfined-aquifer flow equation (McDonald and Harbaugh, 1984):

$$\frac{\partial}{\partial x}\left(h\,K'\,\frac{\partial h}{\partial x}\right) + \frac{\partial}{\partial y}\left(h\,K'\,\frac{\partial h}{\partial y}\right) - W = \frac{\partial h}{\partial t}\,S_y \qquad (6)$$

where

h = saturated thickness of aquifer, in meters;
W = source-sink term, in meters per day;
S_y = aquifer storage coefficient, dimensionless;
x = length coordinate in x direction, in meters; and
y = length coordinate in y direction, in meters.

In this application, hydraulic conductivity (K') is assumed to be isotropic. i was included in the source-sink term (W) and the height of the ground-water mound above the initial water table (h_m) at the center of the test basin was equal to the ponded depth (H') plus the initial water-table depth (L'). The simulated i response to a specified H can be used to calculate τ. The saturated-flow model is described in greater detail in the "Model Development" section.

Simulations of τ in this report are performed using a one-dimensional vertical transient-flow model (eq. 5) for the case where the water table does not intersect the basin floor and a two-dimensional saturated unconfined-aquifer flow model (eq. 6) for the case where a ground-water mound intersects the basin floor. Because different scales were used in the application of the two models, a dilemma arises in choosing an appropriate scale for describing model applications. This occurs because the relatively large spatial intervals for the two-dimensional saturated unconfined-aquifer flow model (eq. 6) are conventionally applied and reported in meters. On the other hand, the one-dimensional vertical transient-flow model (eq. 5) is not practically adaptable to direct use in units of meters without using very small numbers, and the convention of use (including both parameters and output) is almost always in centimeters. Even though output of the vertical transient-flow model could be converted to units of meters, the conversion of all parameters for description of model applications would be much more complex and would result in a presentation of spatial scale that is nonintuitive for the vertical transient-flow model. For this reason, parameters and output for each model are presented and described separately according to the actual spatial scale used in model applications. Because τ is dimensionless, it provides a single consistent unit of comparison for results of the two models. Where direct comparisons are necessary, both scales (centimeters and meters) are used.

METHODS AND MATERIALS

From September 1986 to October 1987, a 15x15-m artificial-recharge test basin was operated within the Garrison Diversion unit irrigation area near Oakes, Dickey County, N.Dak. Subsoil materials ranged from fine to coarse sand, but medium sand was predominant. Between September 1986 and August 1987, three 30-d (day) operational tests were conducted. The first operational test was conducted during September and October 1986 and was followed by full renovation that included excavation and replacement of the test-basin soils to a depth of 60 cm. The second operational test was conducted during May and June 1987 and was followed by natural renovation through 10 d of drying. The third operational test was conducted during June and July 1987. The average suspended-sediment concentration for the influent water ranged from 48 to 60 mg/L during the three operational tests.

Near the end of the first and second operational tests, ponded depth (H) was increased from 60 cm to about 100 cm to evaluate infiltration-rate (i) response to changes in H during rising-head experiment conditions. For the third operational test, H was decreased from 62 cm to 48 cm to evaluate i response to changes in H during falling-head experiment conditions. H then was increased to 84 cm to evaluate a third rising-head experiment. For each experiment, changes in i were determined with discharge measurements taken at the test-basin intake. In addition, i was monitored at four local test-basin sites using pressure head measured on tensiometers placed in the subsoil and unsaturated hydraulic conductivity [$K(S)$] measured at each field site before test-basin operation.

Prior to the first and second operational tests, field methods of Ahuja and others (1980) and Schuh (1988) were used to measure $K(S)$ for soil layers 0 to 8, 8 to 22, 22 to 38, and 38 to 53 cm deep. During test-basin operation, flow calculated from the predetermined $K(S)$ relation of the deepest soil layer (assumed to be unaltered) and the measured hydraulic gradient at that depth were used to monitor changes in $K(S)$ for each overlying soil layer. Details of the method and instruments used to calculate the change in $K(S)$ are described in Schuh (1988). Further details of measurement and interpretation of hydraulic data are described by Schuh and Shaver (1988). $K(S)$ measurement sites, soil-sample sites, and other test-basin monitoring sites for the first operational test are shown in figure 3. Field-monitoring sites were similar for the second and third operational tests. For model 1, a single set of basin soil $K(S)$ field data and soil-water volumetric fraction (θ) laboratory data was selected from site TI4 and is presented in table 1. The data are presented for the selected basin soil both before and after clogging.

Before and after the first operational test, ring samples (3 cm in length by 5 cm in diameter) were obtained from soil layers corresponding in depth to, but 3 m distant from, the soil layers at each of the $K(S)$ measurement sites (fig. 3). Two ring samples were obtained from each depth increment with a sampler described by Schuh (1987). To avoid damage, a buffer volume of soils was left on each end of the ring samples, and each sample was wrapped gently with several layers of aluminum foil secured with masking tape. All final

FIRST OPERATIONAL TEST (FALL 1986)

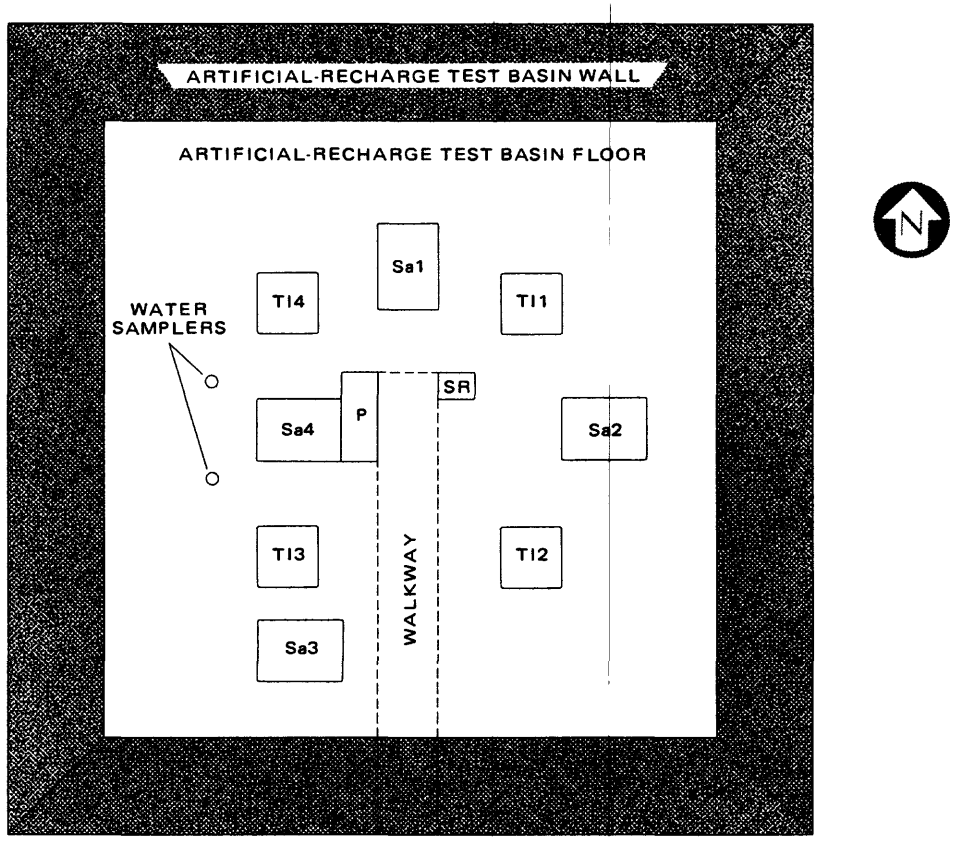

EXPLANATION

TI4 UNSATURATED HYDRAULIC-CONDUCTIVITY MEASUREMENT SITE--Number is site identification number

Sa1 SOIL-SAMPLE SITE--Number is site identification number

P POTENTIOMETER NEST

SR STAGE RECORDER

Figure 3.--Test-basin sampling and instrumentation layout for the first operational test.

Table 1.--Unsaturated hydraulic conductivity and soil-water volumetric fraction of a nonclogged soil and a clogged soil at site TI4 during the first operational test

[S, pore-water pressure head, in centimeters of water; θ, soil-water volumetric fraction, dimensionless; NC, nonclogged soil; $K(S)$, unsaturated hydraulic conductivity, in centimeters per hour; C, clogged soil; --, no data]

S	θ-NC	$K(S)$-NC	θ-C	$K(S)$-C
5	0.3195	11.300	0.3105	2.500
10	.3195	11.300	.3105	2.500
15	.2650	11.300	.2800	2.300
20	.1951	8.000	.2405	1.800
25	.1350	4.390	.1900	1.500
30	.1132	2.750	.1385	.240
35	.1000	1.850	.1200	.060
40	.0879	1.310	.1125	.026
45	.0850	.970	.1050	.007
50	.0874	.739	.1028	.004
60	.0745	.436	.0961	--
80	.0678	.221	.0864	--
100	.0655	.125	.0819	--
120	.0633	.078	.0789	--

trimming of the samples was done in the laboratory. The undisturbed ring samples then were used to determine the laboratory desorption/soil-moisture retention relation according to the pressure-extraction method described by Klute (1986). Soil bulk density was measured according to the core method described by Blake and Hartge (1986).

RESULTS AND DISCUSSION

Field experiments of infiltration-rate (i) response to changes in ponded depth (H) were limited to late stages of test-basin operation when changes in surface impedance caused by clogging of the test-basin soil were minimal. Field-experiment results, therefore, were obtained only for a well-formed impeding surface layer. For the first operational test, H was increased

quickly to avoid confusion with flow-attenuation effects resulting from continued sediment clogging. H was increased by fully opening the gate valve at the test-basin intake. After H was increased, the gate valve was adjusted to an inflow rate corresponding to the calculated maximum infiltration-rate response ratio ($\tau = 1$) for a nondisturbed test-basin floor. A τ value exceeding 3 was measured before the first operational test was terminated. This value indicated a likely disturbance of the surface filter-cake layer by the increased flow of water into the test basin.

Changes in i response caused by increased basin-wall area were considered unlikely because the test-basin walls were covered with polyethylene. As H was increased, however, a large sediment plume was detected near the test-basin intake. The sediment plume indicated likely disturbance of the surface filter-cake layer. Examination of the test-basin floor following termination of the first operational test confirmed scour extending outward from the test-basin intake. Because scoured soil infiltration rates were two to three orders of magnitude larger than unscoured soil rates, a large change in overall i resulted from a relatively small scoured area.

For the second operational test, the gate valve at the test-basin intake was opened more gradually, and a deflection board was placed beneath the intake to avoid turbulence. Increased turbidity extending outward from the test-basin intake again was detected. Results of the second operational test (table 2) indicated that substantial disturbance still was affecting i response to changes in H. Because of differences in tensiometer response times, H and pore-water pressure head (S) at the lower boundary of the surface soil layer were measured at each unsaturated hydraulic-conductivity [$K(S)$] measurement site five times before and five times after the tensiometric response to changes in H. The H and S values measured before the tensiometric response then were averaged to determine the initial ponded depth (H_1) and the initial pore-water pressure head at the lower boundary of the surface filter-cake layer (S_{f1}). The H and S values measured after the tensiometric response were averaged to determine the final ponded depth (H_2) and the final pore-water pressure head at the lower boundary of the surface filter-cake layer (S_{f2}). This method of determining H_1, H_2, S_{f1}, and S_{f2} resulted in slight differences between measurement sites as presented in tables 2 and 3.

The τ value measured at the test-basin intake was larger than the average τ value measured at the four *in-situ* (TI1 to TI4) measurement sites (fig. 3). Of the four *in-situ* measurement sites, the one directly in front of the stilling basin (TI3) exhibited a τ value closest to that obtained at the intake. The two measurement sites at intermediate distance from the stilling basin (TI2 and TI4) exhibited τ values that also were sufficiently large to indicate some scour. The measurement site farthest from the stilling basin (TI1) exhibited a τ value that indicated no scouring was likely. The distribution of these data indicate that the overall increase in i caused by an increase in H was dominated by basin scouring in the area immediately in front of the stilling basin when H was increased.

Table 2.--Infiltration-rate response to changes in ponded depth for the second operational test

[H_1, initial ponded depth, in centimeters; H_2, final ponded depth, in centimeters; S_{f1}, initial pore-water pressure head at lower boundary of surface filter-cake layer, in centimeters of water; S_{f2}, final pore-water pressure head at lower boundary of surface filter-cake layer, in centimeters of water; i_1, initial infiltration rate, in centimeters per hour; i_2, final infiltration rate, in centimeters per hour; η, H_2/H_1, dimensionless; ι, i_2/i_1, dimensionless; τ, ι/η, dimensionless; --, no data; $K(S)$, unsaturated hydraulic conductivity, in centimeters per hour]

Measurement site	H_1	H_2	S_{f1}	S_{f2}	i_1	i_2	η	ι	τ
				Rising-head experiment					
Intake	61	100	--	--	0.460	1.690	1.64	3.67	2.24
TI1	41	72	-37	-34	.014	.017	1.76	1.21	.69
TI2	60	91	-14	-9	.108	.299	1.52	2.77	1.82
TI3	68	107	-19	-17	.022	.074	1.57	3.36	2.14
TI4	62	102	-18	-16	.042	.110	1.65	2.62	1.59
Mean of $K(S)$ measurement sites	58	93	-22	-19	.046	.125	1.62	2.49	1.56
Standard error for $K(S)$ measurement sites	12	16	10	11	.043	.122	.10	.91	.52

Table 3.--Infiltration-rate response to changes in ponded depth for the third operational test

[H_1, initial ponded depth, in centimeters; H_2, final ponded depth, in centimeters; S_{f1}, initial pore-water pressure head at lower boundary of surface filter-cake layer, in centimeters of water; S_{f2}, final pore-water pressure head at lower boundary of surface filter-cake layer, in centimeters of water; i_1, initial infiltration rate, in centimeters per hour; i_2, final infiltration rate, in centimeters per hour; η, H_2/H_1, dimensionless; ι, i_2/i_1, dimensionless; τ, ι/η, dimensionless; --, no data; $K(S)$, unsaturated hydraulic conductivity, in centimeters per hour]

Measurement site	H_1	H_2	S_{f1}	S_{f2}	i_1	i_2	η	ι	τ
				Falling-head experiment					
Intake	62	48	--	--	1.270	0.812	0.77	0.64	0.83
TI1	42	29	-38	-38	.024	.017	.69	.71	1.03
TI2	58	48	0	-15	.205	.160	.83	.78	.94
TI3	66	57	-18	-18	.049	.028	.86	.57	.66
TI4	61	51	-19	-21	.071	.044	.84	.62	.74
Mean of $K(S)$ measurement sites	57	46	-19	-23	.087	.062	.80	.67	.84
Standard error for $K(S)$ measurement sites	10	12	16	10	.081	.066	.08	.09	.17

Table 3.--Infiltration-rate response to changes in ponded depth for the third operational test--Continued

Measurement site	H_1	H_2	S_{f1}	S_{f2}	i_1	i_2	η	ι	τ
				Rising-head experiment					
Intake	46	84	--	--	0.352	0.534	1.83	1.52	0.83
TI1	27	70	-37	-35	.006	.015	2.59	2.50	.97
TI2	46	89	-36	-26	.119	.230	1.93	1.93	1.00
TI3	54	97	-19	-18	.020	.037	1.80	1.85	1.03
TI4	49	92	-21	-17	.023	.044	1.88	1.91	1.02
Mean of $K(S)$ measurement sites	44	87	-28	-24	.042	.082	2.05	2.05	1.00
Standard error for $K(S)$ measurement sites	12	12	9	8	.052	.100	.36	.30	.03

Because of the sensitivity of the test-basin floor to scour, a falling-head experiment (which should not produce scouring currents) was conducted during the third operational test. Results of the falling-head experiment are presented in table 3. Values for τ at the $K(S)$ measurement sites varied from 0.74 to 1.03 and had a mean of 0.84. This mean agreed well with the average τ calculated for the test-basin intake (0.83).

The pore-water pressure head at the lower boundary of the surface filter-cake layer (S_f) became more negative as H decreased because a lower H causes less infiltration through the surface filter-cake layer. Less infiltration through the surface filter-cake layer caused a decrease in soil-water volumetric fraction (θ) beneath the clogged layer. During the falling-head experiment (table 3), two of the four $K(S)$ measurement sites (TI1 and TI3) had S_f changes that were smaller than the detection level for mercury tensiometric measurement. One of the four measurement sites (TI4) had a small S_f change (2 cm), and one (TI2) had a large S_f change (15 cm).

During the rising-head experiment in the third operational test, H was increased gradually to 97 cm. To minimize scour, the deflection board again was placed at the intake, and a small inflow-rate increase was set. The average τ calculated for the test-basin intake (0.83) indicated a response similar to that of the falling-head experiment. Overall scour effects in the rising-head experiment seem to have been minimal.

Results of the rising-head experiment in the third operational test are presented in table 3. Values for τ at the $K(S)$ measurement sites varied from 0.97 to 1.03 and had a mean of 1.00. At sites TI1 and TI2, effects of the rising-head experiment were close to those of the falling-head experiment although the S_f values measured in the rising-head experiment were smaller, indicating that additional surface sealing likely had occurred. At sites TI3 and TI4, the τ values exceeded those measured in the falling-head experiment. Factors influencing effects on sites TI3 and TI4, however, did not seem to be influential over the entire test basin. Subsoil pore pressures increased at each of the $K(S)$ measurement sites.

MODEL DEVELOPMENT

During the fall of 1986 and the spring of 1987, field experiments were conducted at an artificial-recharge test basin to evaluate infiltration-rate (i) response to changes in ponded depth (H). During early stages of test-basin operation, clogging of the test-basin soil caused large decreases in i, and i response to changes in H could not be discerned accurately. For this reason, field experiments were limited to late stages of test-basin operation when changes in i caused by clogging of the test-basin soil were extremely slow and i response to changes in H would not be confused with changes in i caused by surface clogging. Because field experiments were limited to late stages of test-basin operation, i response to changes in H was obtained only for the case of a well-formed impeding surface layer (fig. 2, case A).

Because of field-experiment limitations on time and clogging conditions and because of the desirability of extending interpretations beyond the immediate size and shape of the experimental artificial-recharge test basin, computer models were used to simulate water movement through the basin. Two separate models were used to simulate two conditions. The first model (model 1) consisted of a one-dimensional simulation of unsaturated flow through the clogging basin floor to the water table during conditions of varying surface impedance. The second model (model 2) consisted of a two-dimensional simulation of recharge through the basin floor during conditions when a ground-water mound intersects the basin floor in early stages of basin operation. The objective of both model simulations was to determine i response to changes in H during varying basin conditions rather than quantify recharge through the test basin. Defining actual artificial-recharge quantities through a test basin would be subject to a wide variability in field hydraulic properties and would be of doubtful value. Spatial variability of hydraulic properties was discussed by Schuh (1988) and Schuh and Shaver (1988).

Model 1 (Unsaturated Flow Through an Impeding Surface Layer)

The objective of model 1 simulations was to simulate infiltration-rate (i) response to changes in ponded depth (H) for the initial stages of basin operation. Hydraulic-parameter values for the basin were determined in the field and in the laboratory for periods before and after basin operation. The measured pore-water pressure head (S) at the basin floor was used as the initial upper pressure-boundary condition. A 0-cm S at the water table was used as the lower pressure-boundary condition. Specifying water-table depth (L') can be complicated by ground-water mounding during basin operation. However, for measured experimental clogging conditions, L' variations were limited to a few centimeters. Therefore, S at an average L' of 4 m (400 cm) was used as the lower pressure-boundary condition. Initial S values for each of 42 depth nodes within the simulated subsoil were specified as equal to the node's distance above the water table.

Mathematical Approach

The computer code of Lappala and others (1987) was used to develop a model to simulate infiltration through the subsoil. The code uses a finite-difference method, which solves equations at discrete points rather than continuously, to compute an approximate solution to equation 5.

The accuracy of the approximate solution is affected by the level of spatial and temporal discretization. A total of 42 depth nodes was used in the model simulation. Distance between nodes varied from 0.2 cm below the surface filter-cake layer to 25 cm near the water table.

Temporal discretization was determined more by numerical stability requirements than by desired output. To achieve a stable convergence on the solution for equation 5, very fine resolution [as small as 10^{-7} h (hours)] was required in some simulations of early stages of basin operation. Temporal resolution then was decreased gradually, as model stability allowed, to reduce computer time.

Surface Filter-Cake Layer Impedance Development

Surface filter-cake layer impedance (R_f) is one of the key input parameters required in model 1 simulations. R_f is defined by the following equation:

$$R_f = \frac{L_f}{K}, \tag{7}$$

where

R_f = surface filter-cake layer impedance, in hours;
L_f = thickness of surface filter-cake layer, in centimeters; and hydraulic conductivity (K) is applied to the surface filter-cake layer.

A realistic assessment of the range of R_f values and their relation to clogging of the basin soil surface during the application of turbid water was required to assist in formulating a realistic simulation strategy. To estimate R_f during formation of the surface filter-cake layer, a secondary homogeneous layer of clogging was assumed between the lower surface filter-cake layer boundary (0.1 cm) and 23 cm. For the field hydraulic measurements, the shallowest tensiometer was placed at 7.6 cm. The hydraulic gradient measured for the 7.6- to 23-cm sediment-clogged layer then was extrapolated to 0.1 cm to estimate pore-water pressure head at the lower boundary of the surface filter-cake layer (S_f). The estimated surface filter-cake layer impedance (R_f') then could be calculated with the following equation:

$$R_f' = \frac{(H - S_f + L_f)}{i}. \tag{8}$$

where

R_f' = estimated surface filter-cake layer impedance, in hours; and
S_f = pore-water pressure head at lower boundary of surface filter-cake layer, in centimeters of water.

Equation 8 was derived by algebraically combining the definition for R_f (eq. 7) with Darcy's law (eq. 1) and by applying hydraulic conductivity (K) to the surface filter-cake layer and substituting S_f for the pore-water pressure head (S) and substituting the thickness of the surface filter-cake layer (L_f) for the thickness of the surface soil layer (L_s). L_f was determined by summing the product of flow and suspended solids over time to determine specific deposit, in grams per cubic centimeter, and dividing the specific deposit by the measured bulk density of the surface filter-cake layer (1.22 g/cm^3). Each time the resulting estimated thickness was negligible in relation to the ponded depth (H) and S_f. Final calculations of R_f' versus time were made with the assumption that L_f is approximately equal to zero.

Calculated R_f values for the first operational test are shown in figure 4. The cyclical variations within the overall rising trend of the data correspond to climatic factors influencing tensiometric measurements (i.e., barometric pressure or air temperature) rather than to actual cyclical alterations of the surface filter-cake layer in the process of formation. An approximate maximum R_f' value of 25 h, which corresponds to the R_f' value of a 0.2-cm surface filter-cake layer, was calculated for the first operational test. If K of the surface filter-cake layer soil was constant regardless of the depth of the layer, the maximum R_f value simulated in model 1 (R_f = 1,000 h) would correspond to the R_f value of an 8-cm surface filter-cake layer.

Simulation Strategy

Changes in infiltration-rate (i) response and degree of subsoil saturation were simulated by changing ponded depth (H) from 60 to 120 cm. Hydraulic conditions prior to the change in H were generated by a steady-state flow simulation. The change in i caused by changes in H was estimated by a transient-flow simulation that was conducted until a new steady-state flow regime was achieved.

Soil hydraulic-property values measured at different stages of test-basin clogging were used as input for separate simulations (Schuh, 1988; Schuh and Shaver, 1988). Simulated conditions included: (1) No clogging, (2) sediment clogging to 23 cm and no surface filter-cake layer, (3) sediment clogging to 23 cm and a surface filter-cake layer having 1-h impedance, (4) sediment clogging to 23 cm and a surface filter-cake layer having 10-h impedance, (5) sediment clogging to 23 cm and a surface filter-cake layer having 100-h impedance, and (6) sediment clogging to 23 cm and a surface filter-cake layer having 1,000-h impedance.

The simulation conducted for sediment clogging to 23 cm and no surface filter-cake layer (condition 2) was based on experimental observations of Schuh (1988). Unsaturated hydraulic-conductivity [$K(S)$] data used for the 0- to 23-cm sediment-clogged layer were measured for the clogging process during actual test-basin operation.

Surface filter-cake layer impedance (R_f) was calculated using equation 7. During test-basin operation, the surface filter-cake layer thickened as cumulative sediment load increased. For the first operational test, the final measured thickness of the surface filter-cake layer (L_f) was between 0.1 and 0.2 cm.

Separate steady-state flow simulations were used because development of a single, temporally continuous model would require a valid expression for the relation of R_f to cumulative sediment load. Such expressions are difficult to derive, particularly for early stages of basin operation when sediment is penetrating into the subsoil pores, and likely would not provide greater accuracy for the comparisons delineated in the modeling objective.

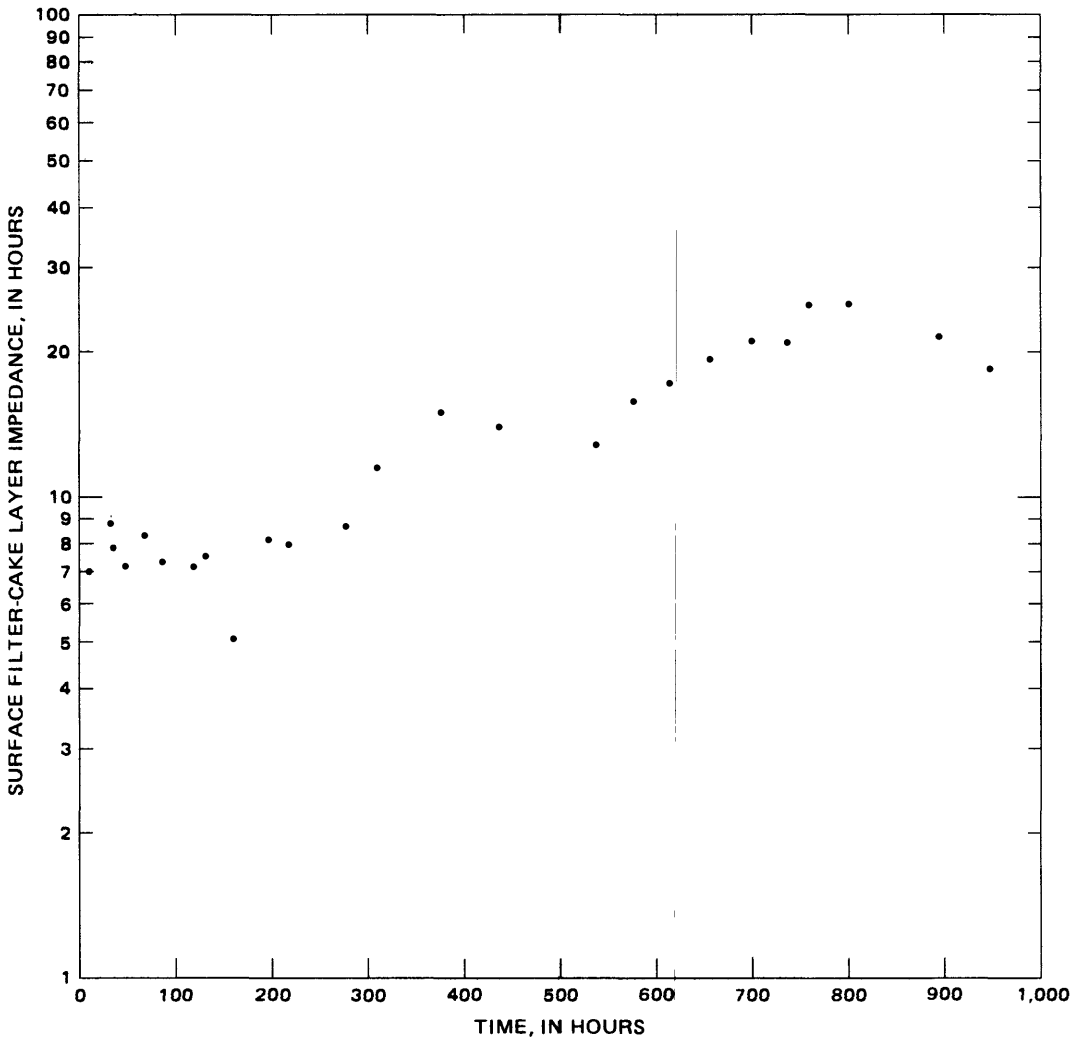

Figure 4.--Calculated surface filter-cake layer impedance values for the first operational test.

Model-Parameter Estimation

Van Genuchten (1980) presented a closed-form functional relation for unsaturated hydraulic conductivity as a function of the soil-water saturation fraction [$K(\theta')$] based on the soil-moisture retention expression:

$$\theta' = \left[\frac{1}{(1 + (a\ S)^n)}\right]^m \tag{9}$$

where

$$\theta' = \frac{(\theta - \theta_r)}{(\theta_s - \theta_r)} \tag{10}$$

where

θ' = soil-water saturation fraction, dimensionless;
m = empirical exponent for van Genuchten water-retention function, dimensionless;
a = empirical factor for van Genuchten water-retention function, in inverse centimeters;
n = empirical exponent for van Genuchten water-retention function, dimensionless;
θ = soil-water volumetric fraction, dimensionless;
θ_r = residual soil-water volumetric fraction, dimensionless; and
θ_s = saturated soil-water volumetric fraction, dimensionless.

The exponents n and m and the factor a are empirically determined. An equation for specific-moisture capacity corresponding to equation 9 is presented in Lappala and others (1987).

The following $K(\theta')$ predictive equation was derived with Mualem's (1976) theory:

$$K(\theta') = K_s\ (\theta')^p\ [1 - (1 - (\theta')^{1/m})^m]^2 \tag{11}$$

where

$K(\theta')$ = unsaturated hydraulic conductivity as a function of soil-water saturation fraction, in centimeters per hour;
K_s = saturated hydraulic conductivity, in centimeters per hour; and
p = a pore-interaction exponent, dimensionless.

For each test-basin operation, the exponents m, n, and p and the factors a, θ_s, and θ_r were optimized for each combined hydraulic-conductivity (K), soil-water saturation fraction (θ'), and pore-water pressure head (S) data set with a FORTRAN computer program (RETC) by Van Genuchten (written commun., no date) based on a Marquardt least-squares parameter-optimization procedure. Although field and laboratory data measured on clean sand before each test-basin operation extended only to an S value of 120 cm, the range of S values

measured during all subsequent operational tests was fully represented. During basin operation, measured soil S values never exceeded 120 cm. Hydraulic parameters determined from field and laboratory measurements are presented in table 4.

Simulated Infiltration-Rate Response (Model 1)

The simulated infiltration-rate (i) response to changes in ponded depth (H) is presented in table 5. Changes in pore-water pressure head at the lower boundary of the surface filter-cake layer (S_f, 0 to 0.1 cm) and in pore-water pressure head at the lower boundary of the sediment-clogged layer (S_s, 0.1 to 23 cm) also are presented. Times for the system to reach steady state after H was increased to 120 cm varied from less than 1 h for the surface filter-cake layer having an impedance value of 1 h to 100 h for the surface filter-cake layer having an impedance value of 1,000 h (fig. 5). Steady state was assumed when model inflow equaled model outflow. For each case, the surface filter-cake layer infiltration rate reached a constant value almost immediately.

The simulated infiltration-rate response ratio (τ = 0.82) interpolated (fig. 6) for a surface filter-cake layer impedance (R_f) value of 25 h agrees well with both the average τ calculated for the test-basin intake (0.83) and the mean τ for the unsaturated hydraulic-conductivity [$K(S)$] measurement sites (0.84) for the falling-head experiment. The simulated response also agrees well with the average τ calculated for the test-basin intake (0.83) for the rising-head experiment. The falling-head experiment τ values would be expected to be slightly lower than the rising-head experiment τ values because of the greater magnitude of the pore-water pressure head (S; including S_f) at lower H. The good agreement occurred despite full renovation of the test basin and two 30-d operational tests between the time soil hydraulic properties used in the model were measured and the time the falling-head and rising-head experiments were conducted.

The relation of τ vs. R_f for the simulated range of R_f values is shown in figure 6. The plotted values for τ are based on the assumption that a groundwater mound does not form. The plotted value of τ for an R_f value of zero was calculated for the specific case of no filter cake. The soil profile is fully saturated and the hydraulic gradient is 1. As R_f values increase, the soil profile desaturates except for the limiting sediment-clogged layers. The result of desaturation is an increased i response to changes in H. The maximum τ occurred for the simulated R_f value of 100 h. τ declined slightly between an R_f value of 100 h and an R_f value of 1,000 h. The greatest changes in τ occurred between an R_f value of 1 h and an R_f value of 10 h.

Water-Table Depth

All computer simulations were for a constant water-table depth (L') of 4 m. A different L' could alter responses. For a deeper water table, a negligible change in the infiltration-rate response ratio (τ) would be expected when the surface filter-cake layer impedance (R_f) value is greater

Table 4.--Hydraulic parameters determined from field and laboratory measurements of soil-water volumetric fraction, pore-water pressure head at the lower boundary of the surface soil layer, and unsaturated hydraulic conductivity before, during, and after the first operational test

[θ_r, residual soil-water volumetric fraction, dimensionless; θ_s, saturated soil-water volumetric fraction, dimensionless; K_s, saturated hydraulic conductivity, in centimeters per hour; a, empirical factor for van Genuchten water-retention function, in inverse centimeters; n, empirical exponent for van Genuchten water-retention function, dimensionless; m, empirical exponent for van Genuchten water-retention function, dimensionless; p, pore-interaction exponent, dimensionless; NC, nonclogged soil; C, clogged soil]

Soil	θ_r	θ_s	K_s	a	n	m	p
NC	0.0896	0.2885	11.3	0.0386	7.52	0.867	-1.09
C	.0710	.2997	2.5	.5754	19.51	.176	-1.86

than 10 h. A more common case, however, is that of a rising water table because of ground-water mound development.

For a rising water table, a negligible change in τ would be expected for an R_f value greater than 10 h provided the water table remains at least 1 m from the basin floor. This expectation is based on the fact that steady vertical flow through a homogeneous soil creates a unit hydraulic gradient that results in a constant pore-water pressure head (S) except for a transition zone near the water table. As long as the transition zone and its larger S does not intersect the lower boundary of the surface filter-cake layer, both S and the thickness of the surface soil layer (L_s, eq. 1) should remain unchanged, resulting in a constant τ value. For an R_f value of 10 h, a constant S is reached within 1 m of the water table (fig. 7). For an R_f value greater than 10 h, the transition zone is considerably less than 1 m.

Table 5.--Simulated infiltration-rate response to a change in ponded depth from 60 to 120 centimeters

[R_f, surface filter-cake layer impedance, in hours; S_{f1}, initial pore-water pressure head at lower boundary of surface filter-cake layer, in centimeters of water; S_{f2}, final pore-water pressure head at lower boundary of surface filter-cake layer; in centimeters of water; S_{s1}, initial pore-water pressure head at lower boundary of sediment-clogged layer, in centimeters of water; S_{s2}, final pore-water pressure head at lower boundary of sediment-clogged layer, in centimeters of water; i_1, initial infiltration rate, in centimeters per hour; i_2, final infiltration rate, in centimeters per hour; η, final ponded depth divided by initial ponded depth, dimensionless; ι, i_2/i_1, dimensionless; τ, ι/η, dimensionless; --, no data]

R_f	S_{f1}	S_{f2}	S_{s1}	S_{s2}	i_1	i_2	η	ι	τ
[1]0	--	--	--	--	--	--	2	--	0.57
[2]0	6	12	6	10	13.00	14.70	2	1.131	.57
1	5	11	-9	2	9.69	12.00	2	1.238	.62
10	1	4	-15	-12	5.23	8.31	2	1.589	.79
100	-23	-21	-20	-18	.84	1.41	2	1.679	.84
1,000	-29	-28	-25	-22	.09	.15	2	1.667	.83

[1]No clogging within the soil profile. τ was calculated directly (without i_1 and i_2) using equation 4. The thickness of the surface soil layer (L_s) was the depth to the aquifer (400 cm in model 1), and both the initial pore-water pressure head at the lower boundary of the surface soil layer (S_1) and the final pore-water pressure head at the lower boundary of the surface soil layer (S_2) were given values of zero, representing the pore-water pressure head (S) values at the surface of the aquifer.

[2]Clogged surface layer. τ was calculated using model 1.

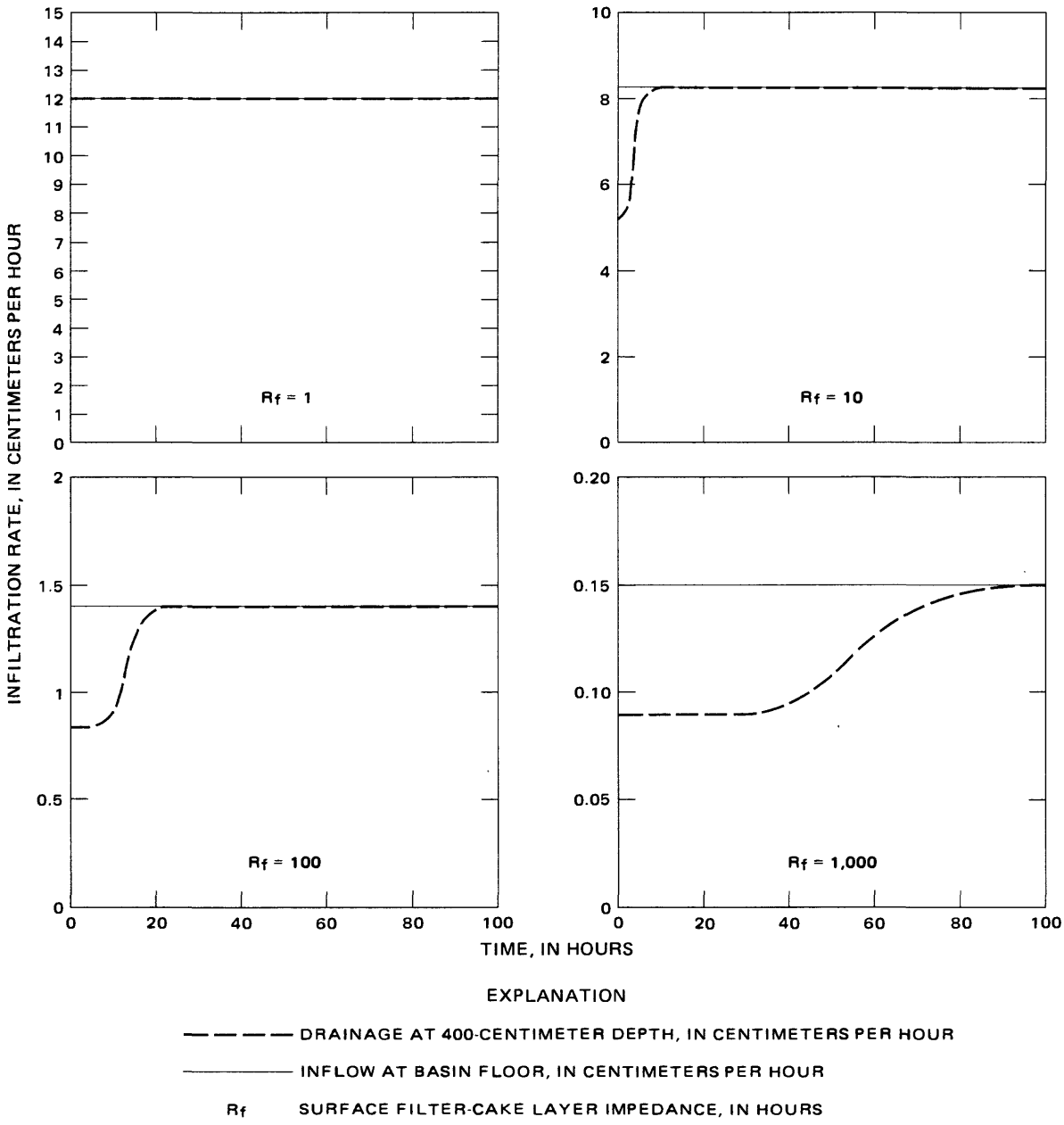

Figure 5.--Simulated steady-state surface infiltration and drainage at the 400-centimeter depth for the specified surface filter-cake layer impedance after increasing ponded depth from 60 to 120 centimeters.

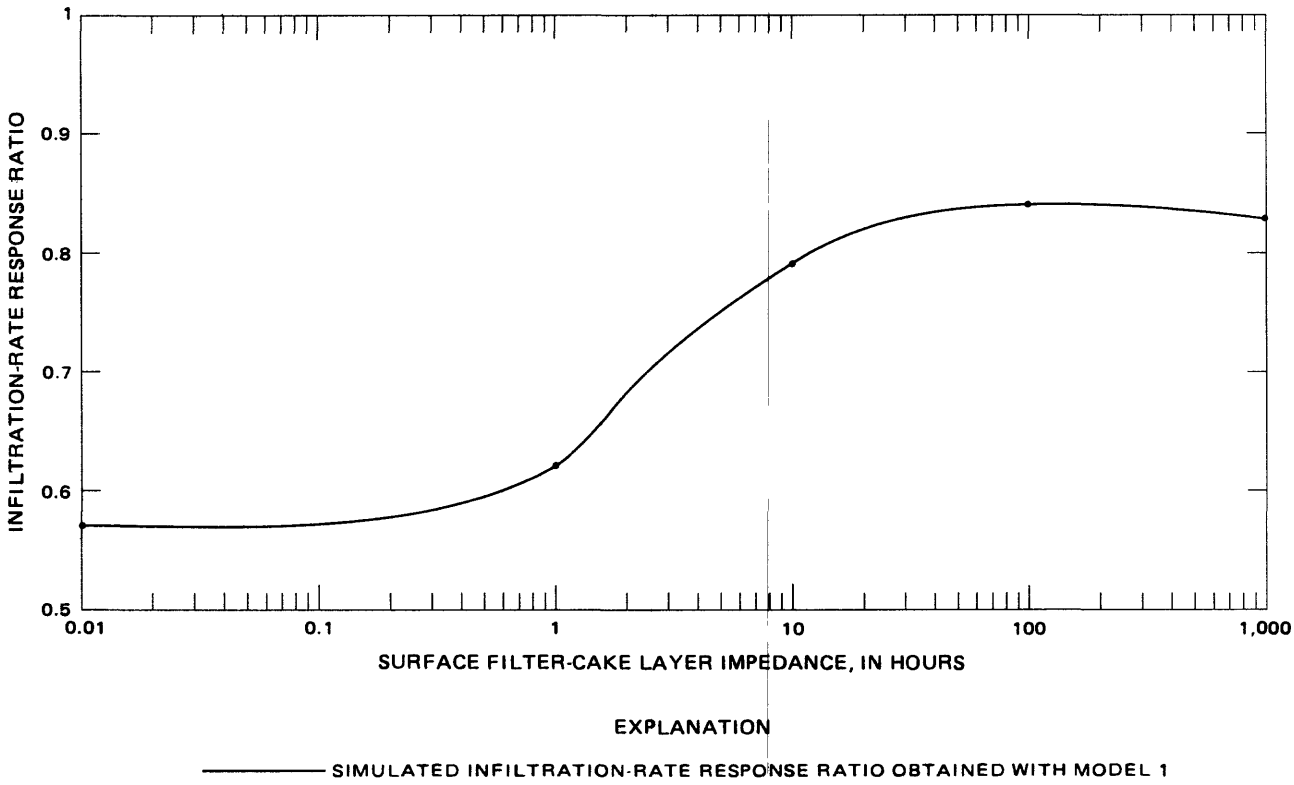

Figure 6.--Infiltration-rate response ratio versus surface filter-cake layer impedance for a simulated basin condition when a ground-water mound does not intersect the basin floor.

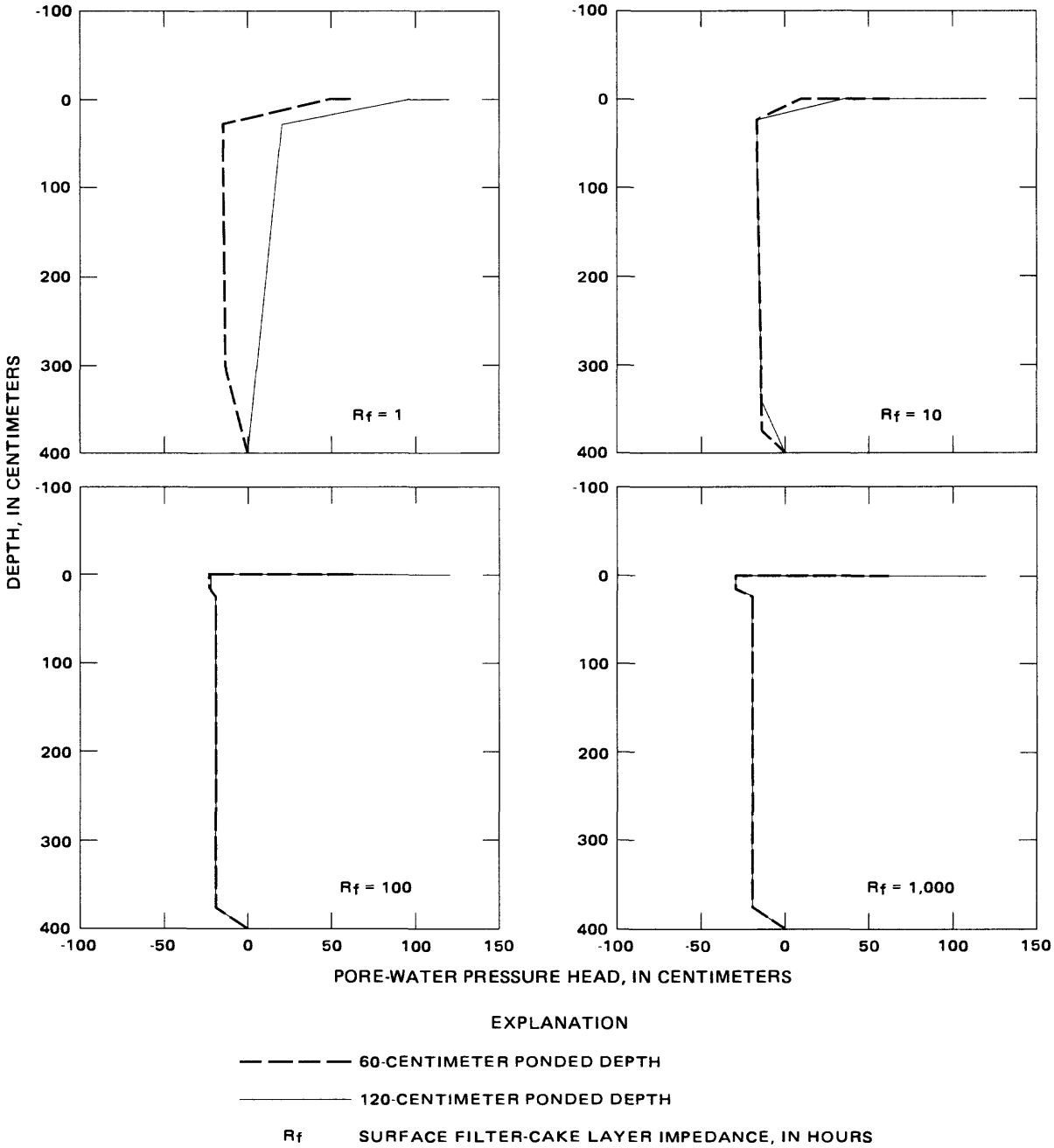

Figure 7.--Simulated steady-state pore-water pressure head distribution with depth for the specified surface filter-cake layer impedance at a 60-centimeter ponded depth and a 120-centimeter ponded depth.

Model 2 (Ground-Water Mound Intersection of Basin Floor During Early Stages of Basin Operation)

The objective of model 2 simulations was to simulate infiltration-rate (I') response to changes in ponded depth (H') during conditions when a ground-water mound intersects the basin floor in early stages of basin operation. The basin recharge rate in model 1 was limited primarily by surface filter-cake layer impedance (R_f). In contrast, the basin recharge rate when a ground-water mound intersects the basin floor is governed by the aquifer's ability to move water laterally away from the basin. Simulations were made for conditions of square and rectangular basin geometries, various basin surface areas, various water-table depths (L'), and various underlying aquifer hydraulic conductivities (K'). Situational and management options simulated are presented in table 6. The movement of the ground-water mound upon intersection with the basin floor was modeled with two-dimensional (areal) saturated unconfined-aquifer flow simulations using the finite-difference code of McDonald and Harbaugh (1984). Two simulations were made for each set of basin geometry, L', and K'--one at a 0.6-m H' and one at a 1.2-m H'. Model nodes within the basin were assigned head values equal to the surface elevation. Model nodes outside the basin were assigned uniform initial head values equal to the water table. Lateral boundaries were placed at a sufficient distance from the basin so as not to be of significance during the 30-d simulation period. In all simulations, the aquifer storage coefficient (S_y) of model nodes outside the basin was 0.25, and the initial saturated thickness of the aquifer (h) was 15.24 m. Because the basin was assumed to be symmetrical, it was necessary to consider only one-fourth of the basin in each model simulation. Total recharge was then four times the simulated flow for the active quadrant.

For each simulation, each of the two lateral directions was divided into 50 node increments. For the 12.4-ha square basin (142 m wide by 142 m long), increments in both directions from the basin center to the basin edge were set at 3 m. From the basin edge, node increments were increased by a factor of 1.2 to an outer boundary 2,003 m from the basin center. For the 12.4-ha rectangular basin (45 m wide by 450 m long), node increments in the width (45 m) direction from the basin center to the basin edge were set at 3.2 m. From the basin edge, node increments were increased by a factor of 1.2 to an outer boundary 37,412 m from the basin center. Node increments in the length (450 m) direction were set at 3 m at the basin edge. From the basin edge, node increments were increased by a factor of 1.2 both inward to the basin center and outward to an outer boundary 8,584 m from the basin center. For the 2.5-ha square basin and the 2.5-ha rectangular basin, node increments were scaled proportionally so that the same number of nodes was used as in the corresponding 12.4-ha basin models. Each simulation consisted of one 30-d stress period divided into 35 time steps. From an initial time step of 0.01 d, the 35 time steps were increased by a factor of 1.2 for each successive time step.

Table 6.--Model 2 simulations of infiltration-rate response to changes in ponded depth (from 0.6 to 1.2 meters) during conditions when a ground-water mound intersects the basin floor in early stages of basin operation

[ha, hectares; L', water-table depth, in meters; K', hydraulic conductivity, in meters per day; i', infiltration rate, in meters per day; τ, infiltration-rate response ratio, dimensionless (initial ponded depth, 0.6 meters; final ponded depth, 1.2 meters)]

Test basin geometry	Test basin surface area (ha)	L'	K'	i'	τ
Square	12.4	1.5	61	0.069	0.65
Rectangular	12.4	1.5	61	.091	.65
Circular[1]	12.4	1.5	61	.054	.64
Square	12.4	3.0	61	.122	.59
Rectangular	12.4	3.0	61	.161	.59
Circular[1]	12.4	3.0	61	.093	.58
Square	12.4	6.0	61	.239	.55
Rectangular	12.4	6.0	61	.316	.55
Circular[1]	12.4	6.0	61	.170	.55
Square	12.4	3.0	31	.076	.59
Rectangular	12.4	3.0	31	.104	.59
Circular[1]	12.4	3.0	31	.057	.58
Square	12.4	3.0	123	.200	.59
Rectangular	12.4	3.0	123	.258	.59
Circular[1]	12.4	3.0	123	.156	.58
Square	2.5	3.0	61	.395	.59
Rectangular	2.5	3.0	61	.491	.59
Circular[1]	2.5	3.0	61	.263	.58

[1]Estimated using constant-drawdown equation.

Simulated Infiltration-Rate Response (Model 2)

The simulated infiltration-rate (i') response to changes in ponded depth (H') for various hydraulic-property and basin-management options is presented in table 6. The infiltration-rate response ratio (τ) indicates that i' response to changes in H' did not vary with basin geometry (square or rectangular), basin surface area (2.5 or 12.4 ha), or aquifer hydraulic conductivity (K'; 31, 61, and 123 m/d). The value of τ for all geometry, surface area, and K' combinations was approximately constant at 0.59 when the initial water-table depth (L') was 3 m. This corresponds to an 18-percent proportional increase in i' that occurs for all simulations, regardless of the initial value of i', when H' is increased from 0.6 to 1.2 m. The 18-percent proportional increase occurs despite a variation in absolute i' values caused by various hydraulic-property and basin-management options.

The 18-percent proportional increase in i' also occurs for the 2.5-ha and the 12.4-ha basins having the same basin geometry and the same aquifer K' values. Absolute i' for the 2.5-ha basin was much larger than absolute i' for the 12.4-ha basin. The 18-percent proportional increase in i' also occurs for all aquifer K' values. Absolute i' values increase in approximate proportion to the log of K' for the three simulated values.

Relative effects of basin design and hydraulic properties on enhanced recharge are of primary interest in this study rather than absolute i' values. Computer simulation of basin-design effects on absolute i' values for the irrigation area near Oakes would not be appropriate because of large spatial variability of the governing soil, aquifer, water, sediment, and climatic properties. The τ value obtained with model 2 for all cases of ground-water mounding when L' was 3 m was 0.59. The τ value obtained with model 1 for the case of no filter cake (saturated vertical flow to the water table) was 0.57. The slight difference between the two τ values was caused by a small change in the simulated L' value [model 1, L' = 4 m (400 cm); model 2, L' = 3 m] for the two models. When L' is properly adjusted, the two τ values are identical. Given a constant L', all simulated cases of recharge through a fully saturated transmission zone resulted in the same i' response to changes in H'.

Effect of Basin Geometry

When a ground-water mound has intersected the basin floor, the driving force for infiltration is the height of the ground-water mound above the initial water table (h_m). Regardless of basin geometry, basin surface area, or aquifer transmissivity (T), infiltration rate (i') increases linearly with h_m. For example, the simulated recharge-rate (I) change in response to changes in h_m for a 12.4-ha square basin overlying an aquifer having a storage coefficient (S_y) of 0.25 and a T of 930 $[(m^3/d)/m^2]m$ is described by the empirical equation

$$I = 4{,}293\ h_m \qquad (12)$$

where

I = recharge rate, in cubic meters per day.

The simulated I change in response to changes in h_m for a 12.4-ha rectangular basin having an S_y of 0.25 and a T of 930 $[(m^3/d)/m^2]m$ is described by the empirical equation

$$I = 5{,}669\ h_m. \qquad (13)$$

The proportionality factor varies with basin geometry as shown in figure 8, but the relation between h_m and I is linear for each case.

Even though I change in response to changes in h_m is linear regardless of basin geometry, the proportionality factor for a rectangular basin is larger than for a square basin (fig. 8), and the proportionality factor for a square basin is larger than for a circular basin. The difference in proportionality factors has two implications: (1) For any given ground-water mound height (provided the mound has intersected the basin floor), total I will be larger for a retangular basin than for a square basin of identical surface area and (2) as ground-water mound height increases, I will increase at a larger absolute rate for a rectangular basin than for a square basin of identical surface area and conducting properties.

In more generalized terms, the basin-geometry effect can be attributed to the difference in the ratios of basin perimeter to basin surface area for square and rectangular basins. A large perimeter per unit surface area allows for fast aquifer transmission of water away from the basin (Baumann, 1965; Hantush, 1967). It can be generalized that the more compact the basin surface, the less I change in response to changes in h_m will be. From this, it is inferred that a circular basin would have a smaller proportionality factor of I change in response to changes in h_m than a square basin of similar size.

Effect of Initial Water-Table Depth

The height of the ground-water mound above the initial water table (h_m) at the center of the basin is equal to the ponded depth (H') plus the water-table depth (L'). Therefore, for the case where a ground-water mound forms quickly, h_m is larger for a larger L'. This means that for any given basin geometry and surface area, if a ground-water mound intersects the basin floor, infiltration rate (i') will be larger if the initial depth of the water table beneath the basin floor is larger. It also follows that if the ground-water mound surface reaches the ponded surface of the basin, then, for any given ground-water mound height and ponded depth, H' must provide a correspondingly smaller proportion of h_m for a larger L'. This means that doubling the initial H' causes a smaller relative change in h_m for a larger L' than for a smaller L'. Because i' is linearly dependent on h_m, the smaller relative change in h_m translates directly to a smaller relative change in i'. Similarly, for a basin having a very small L', doubling H' causes a very large relative increase in i' compared to an initial i'.

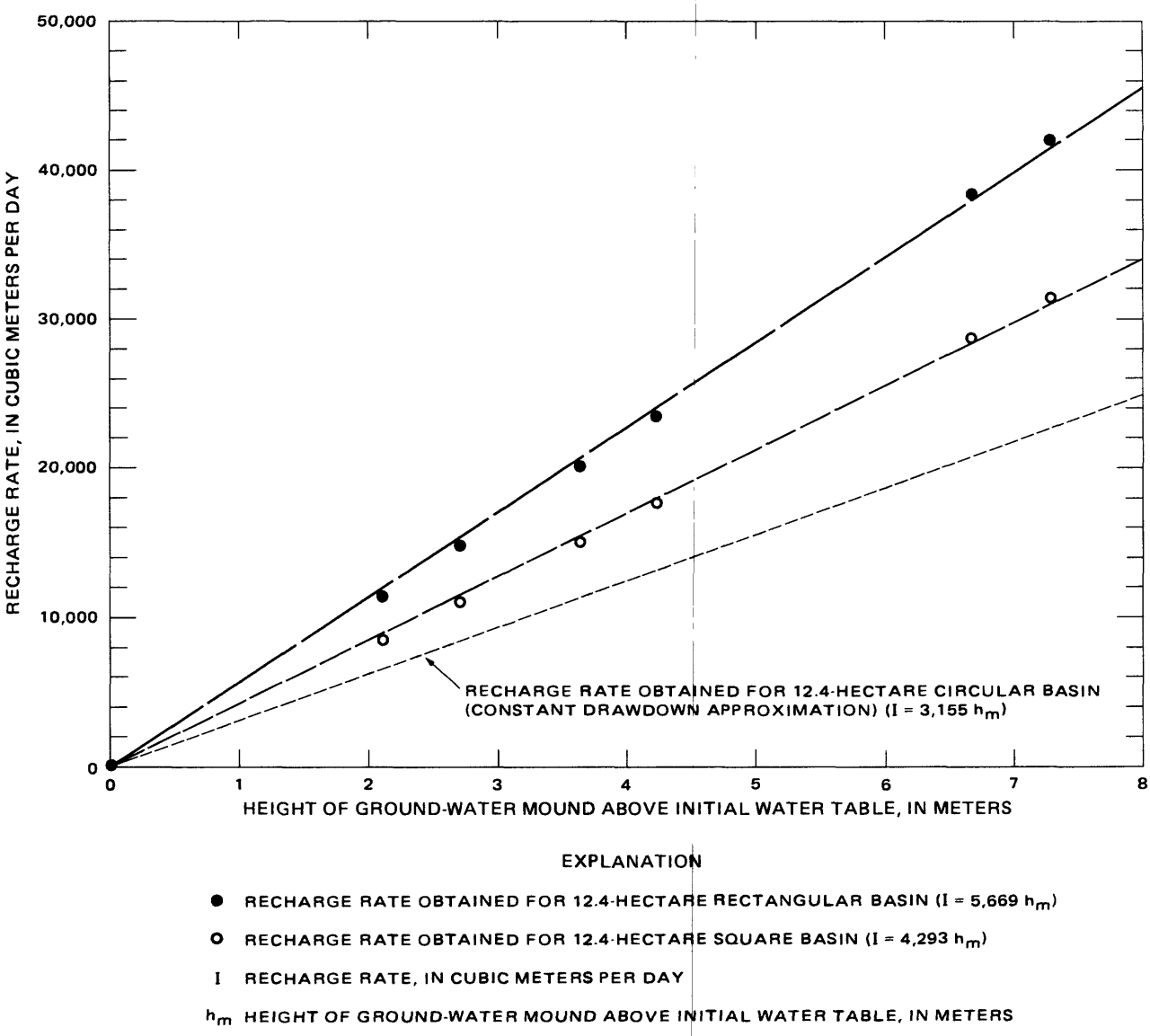

Figure 8.--Recharge rate versus height of ground-water mound above initial water table for simulated infiltration (using model 2 and a constant-drawdown model) through 12.4-hectare square, rectangular, and circular basins having an aquifer storage coefficient of 0.25 and an aquifer transmissivity of 930 cubic meters per day per square meter times meter of aquifer thickness.

The effect of change in L' on the infiltration-rate response ratio (τ) can be evaluated with the empirical equation

$$\tau = 0.6759 - 0.0721 \ln(L') \quad (14)$$

and is shown in figure 9. The use of a 4-m L' in model 2 rather than a 3-m L' would result in a τ value of 0.57, which is identical to the τ value obtained with model 1 for the case of a nonmounded but fully saturated soil between the basin floor and the water table. All simulated cases of recharge through a fully saturated transmission zone resulted in the same τ value, provided L' was the same.

A corollary of the empirical relation shown by equation 14 is that τ should vary with the comparative depth increments of H'. In this study, doubling H' from 0.6 m to 1.2 m was the standard of comparison based on a realistic depth for test-basin construction in the irrigation area near Oakes. However, doubling H' from a much larger initial value of 2 or 3 m would result in a larger proportion of H' in relation to the saturated thickness of the aquifer (h) and a larger i' response to increasing H'. In some cases, basins constructed in old gravel pits are operated with H' exceeding several meters.

Limiting Factors

The operation of basins having a very large ponded depth (H) would seem to be beneficial because of the linear response of infiltration rate (i') to ponded depth (H'). However, there are biological and mechanical factors that limit the practicality of this practice. Soil materials have limited compressive strength; and excessive weight of water can cause collapse of the soil grain matrix and, thus, reduce soil porosity. This is particularly true of organic materials and of soils having large quantities of clay (Bouwer and Rice, 1989). Baumann (1965) suggested a maximum H' of 1.2 m to avoid recharge reduction caused by surface soil compression.

Biological limitations result from the longer water-detention times caused by larger basin water storage during conditions of larger H'. During some climatic and environmental conditions, longer water-detention times enhance algae proliferation, which causes an increase in basin pH through algal photosynthesis. Algal biomass can directly clog the basin surface. In addition, where influent waters are near saturation or oversaturated with solute species having a pH dependent solubility, such as dolomite or calcite, algae activity can cause precipitation of minerals that cement the basin surface and greatly reduce recharge. Algae-induced reduction of recharge has been documented by Bouwer and Rice (1989) and has been detected in the Oakes test basin during late spring and early summer recharge conditions (Schuh, 1990). Bouwer and Rice (1989) have used H' reduction as a means of decreasing water-detention time to minimize algae proliferation and increase basin recharge efficiency. The potential effects of biological factors are highly variable and need to be assessed for each specific basin location and management option.

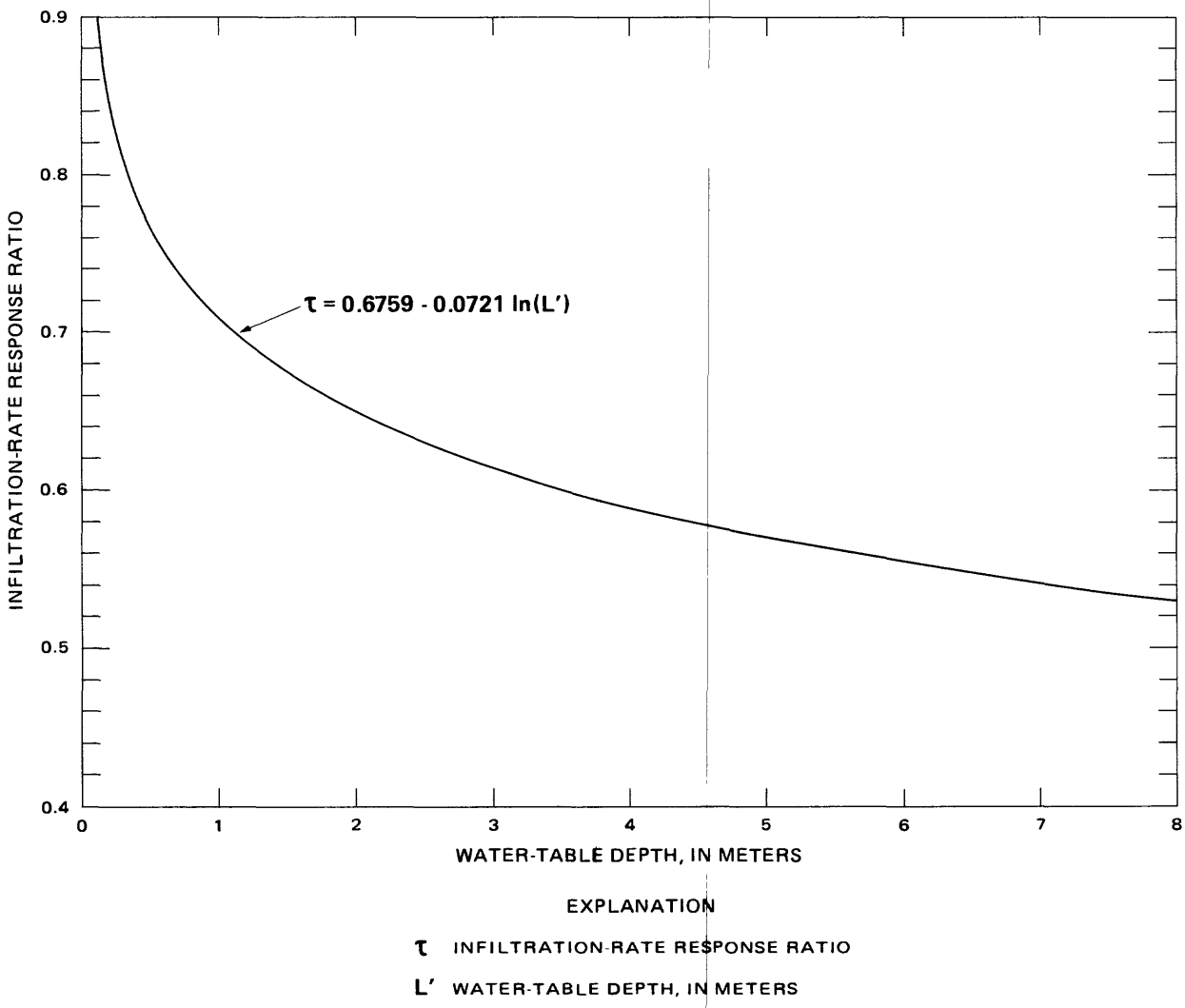

Figure 9.--Infiltration-rate response ratio versus initial water-table depth.

Constant-Drawdown Approximation

For the square and rectangular basins, increasing aquifer transmissivity (T) caused by the rising ground-water mound resulted in a small upward curvature of simulated (model 2) infiltration-rate (i') response for an increasing initial water-table depth (L'). However, the increase in i' response was small, and the linear approximations shown in figure 8 provided a good approximation of the relation between i' response and L'. Because of the linearity, a simplified model having an assumed constant T likely would be adequate for comparison of the relative effectiveness of basin design and hydraulic properties in enhancing i' response. Moreover, because of the insensitivity of the infiltration-rate response ratio (τ) to basin geometry, aquifer hydraulic conductivity (K'), and L', the commonly used equations for calculating T and aquifer storage coefficient (S_y) for conditions of constant drawdown [described by Lohman (1972)] likely would provide an adequate tool for evaluating τ.

The constant-drawdown equation of Lohman (1972) is

$$T = \frac{2.30\ Q}{4\ \Pi\ d} \log\left(\frac{2.25\ T\ t'}{r_w^2\ S_y}\right) \qquad (15)$$

where

T = aquifer transmissivity, in cubic meters per day per square meter times meter of aquifer thickness;
Q = well pumping rate, in cubic meters per day;
t' = time, in days;
d = constant drawdown in a discharging well, in meters; and
r_w = well radius, in meters.

Application of the constant-drawdown equation for analysis of a circular basin is made by considering the elevated ground-water mound as an inverted cone of depression for a pumped well, such that the height of the ground-water mound above the initial water table (h_m) at the center of the basin is used by analogy in place of the constant drawdown in a discharging well (d), the circular basin radius (r_b) is used by analogy in place of the well radius (r_w), and the recharge rate (I) is used by analogy in place of the well pumping rate (Q).

For a circular basin, I response to changes in h_m was determined by substituting h_m for d, r_b for r_w, and I for Q and rearranging equation 15 to solve for I as a function of h_m. For comparison with model 2 applications on the square and rectangular basins (shown in fig. 8), r_b was specified as 263.3 m, the radius of a 12.4-ha circular basin, and time (t') was specified as 30 d, the same as the time specified for model 2 applications. All other parameters of equation 15 were specified the same as for model 2. The resulting equation for I response to changes in h_m is

$$I = 3{,}155\ h_m. \qquad (16)$$

The proportionality factor for a circular basin is shown in figure 8.

The lower rate of linear increase in I response with L' for a circular basin may be caused by the more compact basin geometry as described in comparing the rectangular and square basin relations. A slight difference in the rate of increase also may be caused by the discrete (t' = 30 d) time for I response calculated for the circular basin geometry compared with the 30-d mean value for I response calculated for the rectangular and square basin geometries. Similar calculations were made for all other simulated conditions, and the results are presented in table 6. In all simulated cases, τ values calculated using the constant-drawdown equation were nearly identical to those calculated using model 2. It is concluded that relative i' response to changes in ponded depth (H') for basin-management options and hydraulic-property schemes used in this study could be evaluated adequately with the constant-drawdown equation.

Ponded-Depth Effects on Total Recharge

Because maximum infiltration-rate (i) response to changes in ponded depth (H) occurs during conditions of a large surface impedance when i is small or during conditions of a shallow water-table depth (L') when absolute i is small, it is not practical to design or locate an artificial-recharge basin to enhance i response to changes in H. Rather, it may be more practical to use a larger H to enhance total recharge where limiting factors such as a large surface filter-cake layer impedance (R_f) or a shallow L' cannot be avoided in basin design and location.

The range of potential gains in recharge accomplished by doubling H from 60 to 120 cm [final ponded depth (H_2) divided by initial ponded depth (H_1) equals 2] in a basin in the Oakes area can be approximated using equation 3 and the infiltration-rate response ratio (τ) values from table 5 for the maximum and minimum response cases. When full saturation of the unsaturated zone occurs immediately and is sustained throughout the operational period or when a ground-water mound intersects the basin floor, τ equals 0.57. Using equation 3, the final infiltration rate (i_2) divided by the initial infiltration rate (i_1) equals 1.14. Thus, a minimum increase in total recharge of 14 percent would be expected. When clogging results in immediate and sustained desaturation of the unsaturated zone, τ equals 0.84. Using equation 3, i_2 divided by i_1 equals 1.68. Thus, a maximum increase in total recharge of 68 percent would be expected.

A realistic situation would include a combination of the above increases. A minimum response would occur for the period of large flow rates before clogging of the basin floor and desaturation of the basin subsoil. A maximum response would occur for the period of diminished flow rates following clogging of the basin floor and desaturation of the basin subsoil. Ignoring the intermediate τ values, which would be transitory, the following approximation is made for overall gains in recharge accomplished by doubling H during the first operational test.

During the first operational test, tensiometer measurements at a depth of 7.6 cm indicated that desaturation of the test-basin soil began about 187 h after initiation of test-basin operation. Recharge for the first 187 h of basin operation was 21.3 m when *H* was 60 cm. Applying the minimum increase in recharge of 14 percent caused by doubling *H* from 60 to 120 cm during the period of subsoil saturation, a total recharge of 24.3 m would be predicted for an identical time period. Recharge from 187 to 790 h was 9.1 m when *H* was 60 cm. Applying the maximum increase in recharge of 68 percent caused by doubling *H* from 60 to 120 cm following desaturation of the basin subsoil, a total recharge of 15.3 m would be predicted for an identical time period. The 39.6 m of recharge predicted for the entire operational period when *H* was 120 cm is about 30 percent more than the 30.4 m of recharge measured during test-basin operation when *H* was 60 cm.

During the second operational test, tensiometer measurements at a depth of 7.6 cm indicated that desaturation of the test-basin soil occurred immediately upon initiation of test-basin operation. Calculations made on the basis of hydraulic evidence alone, as for the first operational test, indicate that increased *H* would be highly beneficial during conditions of early desaturation and would result in a 57-percent increase in total recharge. The clogging conditions causing the large *i* response to changes in *H* (carbonate cementation at the test-basin floor) were shown to decrease total recharge (Schuh, 1990).

In calculating infiltration-rate increases, the assumption was made that physical, biological, and chemical effects detrimental to recharge are not caused by doubling *H* from 60 to 120 cm. This is not always the case. Because of potential consolidation, algal biomass clogging, and basin-floor cementation caused by an increase in *H*, the use of a larger *H* as a recharge enhancement tool must be monitored carefully and evaluated whenever it is applied.

CONCLUSIONS

Field experiments and computer simulations of infiltration-rate response to changes in ponded depth were used to evaluate the effectiveness of increasing ponded depth to enhance total recharge to the Oakes aquifer, southeastern North Dakota. A computer model (model 1) was used to simulate the effects of basin clogging and of increasing surface filter-cake layer impedance on infiltration-rate response to changes in ponded depth for the case of an unsaturated soil between the basin floor and the water table or a fully saturated soil between the basin floor and the water table. A second model (model 2) was used to simulate the effect of various basin geometries, basin surface areas, initial water-table depths, and aquifer hydraulic conductivities on infiltration-rate response to changes in ponded depth when a ground-water mound forms quickly and intersects the basin floor. An infiltration-rate response ratio (τ) was used to compare infiltration-rate response to changes in ponded depth for various basin operations.

Field experiments and model 1 computer simulations using soil hydraulic-property values measured at different stages of test-basin clogging indicated that, regardless of water-table depth (provided the water table is deeper than the capillary-fringe length beneath the test-basin floor), the maximum τ (0.84) occurred for a surface filter-cake layer impedance value of 100 hours. For no surface filter-cake layer and when the hydraulic gradient was equal to 1 and the water-table depth was equal to 4 meters, infiltration-rate response to doubling ponded depth from 60 to 120 centimeters (0.6 to 1.2 meters) was only 14 percent (τ = 0.57). Infiltration-rate response increased to 24 percent (τ = 0.62) for a surface filter-cake layer impedance value of 1 hour and then to 58 percent (τ = 0.79) for a surface filter-cake layer impedance value of 10 hours. Infiltration-rate response to doubling ponded depth reached a maximum of 68 percent (τ = 0.84) for a surface filter-cake layer impedance value of 100 hours and decreased slightly to 64 percent (τ = 0.82) for a surface filter-cake layer impedance value of 1,000 hours.

Model 2 computer simulations for the case of a ground-water mound intersecting the basin floor during early stages of basin operation indicated that the relative infiltration-rate response to doubling ponded depth was linearly dependent on the initial water-table depth. Simulated infiltration-rate response to changes in ponded depth did not vary with basin geometry (rectangular, square, or circular), basin surface area (2.5 or 12.4 hectares), or aquifer hydraulic conductivity (100, 200, or 400 centimeters per hour). The proportional increase in infiltration-rate response for all simulations was 18 percent (τ = 0.59) when the thickness of the unsaturated zone was 3 meters. When the initial water-table depth was adjusted to 4 meters, the infiltration-rate response was identical to that of the model 1 computer simulation for vertical transient flow.

Even though the proportional increase in infiltration-rate response to doubling ponded depth did not vary with basin geometry, basin surface area, or aquifer hydraulic conductivity, absolute infiltration-rate response did vary. More total recharge was effected by less compact basin geometries (circular, square, and rectangular in order of increasing recharge); smaller basin surface areas and larger aquifer hydraulic conductivities also increased recharge per unit of surface area.

In general, conditions that lead to an effective infiltration-rate response to changes in ponded depth are least conducive to enhanced total recharge. When a ground-water mound has not intersected the basin floor, the proportional increase in infiltration-rate response to changes in ponded depth is largest for a heavily clogged basin having a large surface impedance, which corresponds to an extremely slow infiltration rate. When a ground-water mound has intersected the basin floor, infiltration-rate response to changes in ponded depth is largest when the initial water-table depth is shallow. However, the case of a shallow initial water-table depth also corresponds to slow infiltration rates when compared with larger water-table depths.

It is not desirable to select a site or design an artificial-recharge basin for maximum effectiveness of use of basin depth as a management tool. However, where certain external conditions (large surface impedance or shallow water table depths) cannot be avoided, increasing basin ponded depth can be an effective but limited means of increasing total recharge. The limiting factors are: (1) The potential consolidation of the soil grain matrix and the loss of soil porosity because of the excessive weight of water during large ponded depths on soils of low compressive strength, and (2) the potential biological clogging caused by increased water-detention times during conditions of larger ponded depth. The effects of the biological limitations must be evaluated and monitored for each location to ensure optimal efficiency.

REFERENCES

Ahuja, L.R., Green, R.E., Chong, S.K., and Nielsen, D.R., 1980, A simplified functions approach for determining soil hydraulic conductivities and water characteristics *in situ*: Water Resources Research, v. 16, p. 947-953.

Allison, L.F., 1947, Effect of microorganisms on permeability of soil under prolonged submergence: Soil Science, v. 63, p. 439-450.

Baumann, P., 1965, Technical developments in ground-water recharge, *in* Chow, V.T., ed., Advances in hydroscience: New York, Academic Press, Inc., v. 2, p. 209-279.

Blake, G.R., and Hartge, K.H., 1986, Bulk density, *in* Klute, A., ed., Methods of soil analysis, part 1, 2nd edition: Agronomy, v. 9, p. 363-375.

Bouwer, H., 1969, Theory of seepage from open channels, *in* Chow, V.T., ed., Advances in hydroscience: New York, Academic Press, Inc., v. 5, p. 121-172.

Bouwer, H., and Rice, R.C., 1989, Effect of water table depth in groundwater recharge basins on infiltration rate: American Society of Civil Engineers, Journal of Irrigation and Drainage Division, 102 p.

Dilyunas, I.P., 1976, Experience in artificial ground-water recharge for water supply in Lithuania: Soviet Hydrology, Selected Papers, v. 15, p. 340-343.

Goss, D.W., Smith, S.J., Steward, B.A., and Jones, O.R., 1973, Fate of suspended sediment during basin recharge: Water Resources Research, v. 9, p. 668-674.

Hantush, M.S., 1967, Growth and decay of groundwater mounds in response to uniform percolation: Water Resources Research, v. 14, p. 844-856.

Huff, G.F., and Wald, J.D., 1989, Geochemistry of artificial recharge tests in the Oakes aquifer near Oakes, southeastern North Dakota: U.S. Geological Survey Water-Resources Investigations Report 89-4122, 74 p.

Jones, O.R., Goss, D.W., and Schneider, A.D., 1974, Surface plugging during basin recharge with turbid water: Transactions of the American Society of Agricultural Engineers, v. 17, p. 1011-1019.

Klute, A., 1986, Water retention: Laboratory methods, *in* Klute, A., ed., Methods of soil analysis, part 1, 2nd edition: Agronomy, v. 9, p. 635-662.

Lappala, E.G., Healy, R.W., and Weeks, E.P., 1987, Documentation of computer program VS2D to solve the equations of fluid flow in variable saturated porous media: U.S. Geological Survey Water-Resources Investigations Report 83-4099, 184 p.

Lohman, S.W., 1972, Ground-water hydraulics: U.S. Geological Survey Professional Paper 708, 70 p.

McDonald, M.G., and Harbaugh, A.W., 1984, A modular three-dimensional finite-difference ground-water flow model: U.S. Department of the Interior, U.S. Geological Survey, National Center, Reston, Virginia.

Mualem, Y., 1976, A new model for predicting the hydraulic conductivity of unsaturated porous media: Water Resources Research, v. 12, p. 513-522.

Nevo, Z., and Mitchell, R., 1967, Factors affecting biological clogging of sands associated with ground water recharge: Water Resources Research, v. 10, p. 231-236.

Schuh, W.M., 1987, Apparatus for extraction of undisturbed samples on noncohesive subsoils: Soil Science Society of America Journal, v. 51, p. 1678-1679.

-----1988, *In-situ* method for monitoring layered hydraulic impedance development during artificial recharge with turbid water: Journal of Hydrology, v. 101, p. 173-179.

-----1990, Seasonal variation of clogging of an artificial recharge basin in a northern climate: Journal of Hydrology, v. 121, p. 193-215.

Schuh, W.M., and Shaver, R.B., 1988, Feasibility of artificial recharge to the Oakes aquifer, southeastern North Dakota: Evaluation of experimental recharge basins: North Dakota State Water Commission Water-Resources Investigation No. 7, Bismarck, North Dakota, 248 p.

Shaver, R.B., 1989, Feasibility of artificial recharge to the Oakes aquifer, southeastern North Dakota: Preliminary cost analysis of a project-scale well field and artificial-recharge facilities: North Dakota State Water Commission Water-Resources Investigation No. 8, Bismarck, North Dakota, 113 p.

Shaver, R.B., and Hove, M.D., 1990, Feasibility of artificial recharge to the Oakes aquifer, southeastern North Dakota: Ground-water data: North Dakota State Water Commission Water-Resources Investigation No. 6, v. 1 and 2, Bismarck, North Dakota, 420 p.

Shaver, R.B., and Schuh, W.M., 1990, Feasibility of artificial recharge to the Oakes aquifer, southeastern North Dakota: Hydrogeology of the Oakes aquifer: North Dakota State Water Commission Water-Resources Investigation No. 5, Bismarck, North Dakota, 123 p.

Suter, M., and Harmeson, R.H., 1960, Artificial ground-water recharge at Peoria, Illinois: Bulletin 48, State Water Survey Division, Urbana, Illinois.

Van Genuchten, M.Th., 1980, A closed-form equation for predicting the hydraulic conductivity of unsaturated soils: Soil Science Society of America Journal, v. 44, p. 892-897.

GLOSSARY OF TERMS

a, empirical factor for van Genuchten water-retention function, in inverse centimeters.

$c(s)$, specific-moisture capacity, in inverse centimeters.

d, constant drawdown in a discharging well, in meters.

h, saturated thickness of aquifer, in meters.

h_i, saturated thickness of underlying aquifer before ground-water mound formation, in meters.

h_m, height of ground-water mound above initial water table, in meters.

H, ponded depth, in centimeters.

H', ponded depth, in meters.

H_1, initial ponded depth, in centimeters.

H_2, final ponded depth, in centimeters.

i, infiltration rate, in centimeters per hour.

i', infiltration rate, in meters per day.

i_1, initial infiltration rate, in centimeters per hour.

i_2, final infiltration rate, in centimeters per hour.

I, recharge rate, in cubic meters per day.

K, hydraulic conductivity, in centimeters per hour.

K', hydraulic conductivity, in meters per day.

$K(S)$, unsaturated hydraulic conductivity, in centimeters per hour.

$K(\theta')$, unsaturated hydraulic conductivity as a function of soil water saturation fraction, in centimeters per hour.

K_s, saturated hydraulic conductivity, in centimeters per hour.

L, thickness of unsaturated zone, in centimeters.

L', water-table depth, in meters.

L_f, thickness of surface filter-cake layer, in centimeters.

L_h, distance from center of channel to position where ground-water mound height effects are negligible, in meters.

L_s, thickness of surface soil layer, in centimeters.

m, empirical exponent for van Genuchten water-retention function, dimensionless.

n, empirical exponent for van Genuchten water-retention function, dimensionless.

p, pore-interaction exponent, dimensionless.

Q, well pumping rate, in cubic meters per day.

R_f, surface filter-cake layer impedance, in hours.

R_f', estimated surface filter-cake layer impedance, in hours.

r_b, circular basin radius, in meters.

r_w, well radius, in meters.

S, pore-water pressure head, in centimeters of water.

S_1, initial pore-water pressure head at lower boundary of surface soil layer, in centimeters of water.

S_2, final pore-water pressure head at lower boundary of surface soil layer, in centimeters of water.

S_f, pore-water pressure head at lower boundary of surface filter-cake layer, in centimeters of water.

S_{f1}, initial pore-water pressure head at lower boundary of surface filter-cake layer, in centimeters of water.

S_{f2}, final pore-water pressure head at lower boundary of surface filter-cake layer, in centimeters of water.

S_s, pore-water pressure head at lower boundary of sediment-clogged layer, in centimeters of water.

S_{s1}, initial pore-water pressure head at lower boundary of sediment-clogged layer, in centimeters of water.

Ss_2, final pore-water pressure head at lower boundary of sediment-clogged layer, in centimeters of water.

GLOSSARY OF TERMS, Continued

S_y, aquifer storage coefficient, dimensionless.

t, time, in hours.

t', time, in days.

T, aquifer transmissivity, in cubic meters per day per square meter times meter of aquifer thickness.

W, source-sink term, in meters per day.

W_b, width of channel at bottom of ponded water, in meters.

W_s, width of channel at surface of ponded water, in meters.

x, length coordinate in x direction, in meters.

y, length coordinate in y direction, in meters.

z, depth coordinate, in centimeters.

η, final ponded depth divided by initial ponded depth, dimensionless.

ι, final infiltration rate divided by initial infiltration rate, dimensionless.

θ', soil-water saturation fraction, dimensionless.

θ, soil-water volumetric fraction, dimensionless.

θ_r, residual soil-water volumetric fraction, dimensionless.

θ_s, saturated soil-water volumetric fraction, dimensionless.

τ, infiltration-rate response ratio (ι/η), dimensionless.